Modeling gasodynamic vortex cooling

A. E. Allahverdyan[1] and S. Fauve[2]

[1]*Yerevan Physics Institute, 2 Alikhanian Brothers Street, 375036 Yerevan, Armenia*

[2]*Laboratoire de Physique Statistique, École Normale Supérieure, PSL Research University; UPMC, Sorbonne Universités; Université Paris Diderot, Sorbonne Paris-Cité; and CNRS, 24 Rue Lhomond, 75005 Paris, France*

(Received 1 March 2017; published 23 August 2017)

We aim at studying gasodynamic vortex cooling in an analytically solvable, thermodynamically consistent model that can explain limitations on the cooling efficiency. To this end, we study an angular plus radial flow between two (coaxial) rotating permeable cylinders. Full account is taken of compressibility, viscosity, and heat conductivity. For a weak inward radial flow the model qualitatively describes the vortex cooling effect, in terms of both temperature and the decrease of the stagnation enthalpy, seen in short uniflow vortex (Ranque) tubes. The cooling does not result from external work and its efficiency is defined as the ratio of the lowest temperature reached adiabatically (for the given pressure gradient) to the lowest temperature actually reached. We show that for the vortex cooling the efficiency is strictly smaller than 1, but in another configuration with an outward radial flow, we find that the efficiency can be larger than 1. This is related to both the geometry and the finite heat conductivity.

DOI: 10.1103/PhysRevFluids.2.084102

I. INTRODUCTION

Air swirling through a cylindrical tube achieves temperature separation: Next to the swirling axis the temperature is lower than the input temperature T_0, while far from the axis it is higher than T_0. This is the vortex cooling-heating effect discovered by Ranque more than 80 years ago [1,2] (see [3–6] for reviews). A temperature separation without cooling was observed also in highly pressurized water [7]. An overall cooling (both output temperatures lower than T_0) was seen for certain vortex tubes [8].

Coolers based on the Ranque effect are convenient in specific applications, e.g., because they do not have moving parts. However, their efficiency is smaller than 1. Much effort was devoted to increasing it, but the best efficiency is still $\simeq 0.6$ [4,6].

The flow inside the Ranque tube is highly complex: It is essentially three dimensional and turbulent. Two configurations have been used: counterflow and uniflow [3–6]. In counterflow vortex tubes the output flows are collected from two different ends of the cylinder: The cold air is extracted from a small aperture around the axis and close to the injection point, while the hot air comes out from the opposite end of the cylinder without being collimated close to the axis [3–6]. Such tubes have both radial [3,4,9] and axial temperature separation [5,10–13]. In the uniflow situation the air is injected circumferentially at one end of the tube and both output flows are collected from the opposite end [3,14]. This radial temperature separation takes place close to the injection point of the air [15].

The full theory of the Ranque effect is elusive; there are several different approaches that attempt to describe the complex three-dimensional flow inside the tube [16–26]. In particular, it is unclear what the minimal ingredients needed to describe the effect are.

Given the complexity of the original Ranque effect and the necessity of understanding general limitations on the efficiency of gasodynamic cooling, it is desirable to come up with a simpler cooling setup, where the complexities of the original Ranque effect are deliberately omitted. The quest for such a simplification was already considered in Ref. [27], where Savino and Ragsdal reported on an experimental realization of a short uniflow tube, where the flow is injected from the surface via a permeable rotating wall and the colder air is collected from the axis [27]. Axial separation of temperature is absent and the whole outgoing flow is cooled [27].

Guided by this experiment, we aim at understanding the phenomenon of vortex, and more general gasodynamic, cooling on a possibly simple theoretical model. We focus on a compressible angular

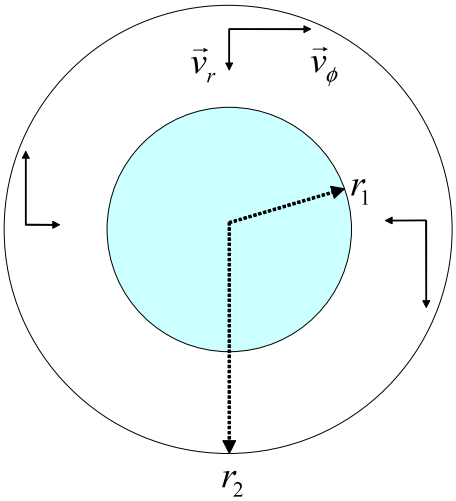

FIG. 1. Cross section of the flow. Two coaxial permeable cylinders with radii r_1 and r_2 rotate with prescribed speeds. Solid vectors $\vec{v}_\phi = v_\phi \vec{e}_\phi$ and $\vec{v}_r = v_r \vec{e}_r$ refer to the velocity components of the flow for $r_1 < r < r_2$. Here the radial flow is directed from the outer (larger) cylinder to the inner (smaller) cylinder. Now $|\vec{v}_r| < |\vec{v}_\phi|$, since the radial flow has to be smaller for cooling.

flow between two rotating cylinders plus a radial motion via permeable cylinder walls (see Fig. 1). We work with a compressible flow, because experimental angular velocities are nearly sonic [4,27]. Moreover, once we are interested by thermodynamic aspects (i.e., cooling efficiency), it is desirable to work in the compressible situation, where the thermodynamic description of the flow is complete and consistent.[1] We assume that the flow is viscous, because (according to Bernoulli's theorem) the adiabatic motion of the fluid does not predict cooling in terms of stagnation enthalpy. However, precisely, such cooling is observed experimentally [27].[2] Hence viscosity is important [6] and then heat conductivity is to be accounted for simultaneously with viscosity, because the Prandtl number of air is close to 1 in both laminar and turbulent regimes.

Our first result is that in the stationary regime of a weak radial flow and a quasisolid angular (vortical) motion, the model predicts cooling in terms of both thermodynamic temperature and stagnation enthalpy. The efficiency of this cooling is smaller than 1. This qualitatively agrees with experiments [27]. The agreement is achieved by using effective (turbulent or eddy) values of viscosity and heat conductivity in the laminar flow model. Such an approach is well known [29]. Using turbulent diffusivities is crude but provides qualitative results [22–24] that allow a theoretical understanding of the cooling effect.

The model predicts a stronger cooling effect for (radially) outward flow of fluid. The unique feature of this effect is that its cooling efficiency is larger than 1, i.e., the pressure gradient is employed more efficiently than for the adiabatic process. This effect agrees with the second law and it is possible due to heat conductivity.

The scenarios of cooling studied here do not amount to refrigeration, i.e., they are not achieved by investing an external work. Naturally, they also do not result from boundaries maintained at low temperature by a heat bath; to ensure this we need to pay special attention to boundary conditions. Hence cooling efficiency is defined as the ratio of the lowest temperature reached adiabatically (for the given pressure gradient) to the lowest temperature actually reached.

---

[1]The incompressible limit is singular from the viewpoint of thermodynamics [28]. Despite the widespread usage of this limit, its consistent thermodynamics was developed only recently [28].

[2]Thus adiabatic theories of the Ranque effect [16–20] do not describe the full cooling effect [21].

Cylindrical vortices with radial flow were already studied in Refs. [23,25,26,30–37], but the problem of finding cooling scenarios with proper boundary conditions was not posed. Dornbrand [25] and later on Pengelley [26] studied the problem precisely having the same purpose as us: to get a solvable model for vortex cooling. However, they did not account for boundary conditions and heat conduction and thus did not obtain proper cooling. Pengelley proposed a necessary condition for cooling that relates to the work done by viscous forces [26]. Below we show that under certain additional limitations this condition is indeed able to produce cooling. References [22–24] used simplified turbulence theories of various types that account for radial heat conductivity and viscous vortex motion. A related but more complete turbulent theory that also accounts for axial motion was given in Ref. [30]. References [31,33,35,36] focus on a laminar flow in the incompressible limit (but they account for axial motion). As our analysis shows, compressibility does not need to be large, but retaining it, and hence allowing for the proper coupling between thermodynamics and mechanics, is necessary for the proper theoretical description of cooling. Reference [32] did not employ the incompressible limit, but studied the problem without the outer cylinder. Several studies on convective heat transfer between concentric cylinders are reviewed in [38–40].

The paper is organized as follows. The next section defines the problem and sets notation and dimensionless parameters. There we also discuss general limitations (in particular, on the cooling efficiency) imposed by the first and second laws. Section III focuses on the definition of cooling, which is not trivial (especially for permeable walls) and thus demands clarification. Cooling scenarios of inward radial flow are studied in Sec. IV. The extent to which these scenarios agrees with experiments is discussed in Sec. V. Section VI discusses the cooling of outward radial flow and shows that its efficiency is larger than 1. A summary is given in Sec. VII. Several technical questions are relegated to the Appendixes.

II. MODEL

A. Navier-Stokes equation

The flow between two rotating concentric cylinders is described via cylindric coordinates (r,ϕ,z) and $\vec{v} = (v_r, v_\phi, v_z)$ are components of the velocity. We assume that all the involved quantities depend only on r, e.g., $\vec{v} = \vec{v}(r)$. We also assume that $v_z = 0$, since in the context of our problem it is useless to keep $v_z \neq 0$ if it is a function of r only. A schematic representation of the flow is displayed in Fig. 1.

In the stationary regime the Navier-Stokes equations for v_r and v_ϕ read [29]

$$\rho\left(v_r\frac{dv_r}{dr} - \frac{v_\phi^2}{r}\right) = -\frac{dp}{dr} + \left(\zeta + \frac{4\eta}{3}\right)\frac{d}{dr}\left[\frac{1}{r}\frac{d(rv_r)}{dr}\right], \tag{1}$$

$$\rho\left(v_r\frac{dv_\phi}{dr} + \frac{v_r v_\phi}{r}\right) = \eta\left(\frac{1}{r}\frac{d}{dr}\left[r\frac{dv_\phi}{dr}\right] - \frac{v_\phi}{r^2}\right), \tag{2}$$

where p is pressure, η and ζ are viscosities, and ρ is the mass density (see Table I). We assume that η and ζ are constants, i.e., they do not depend on p, ρ, or T. Conservation of mass reads ($\vec{\nabla}$ is the gradient)

$$\partial_t\rho + \vec{\nabla}(\rho\vec{v}) = r^{-1}\frac{d}{dr}(\rho r v_r) = 0, \tag{3}$$

$$\rho r v_r = c = \text{const}, \tag{4}$$

where c (a positive or negative constant) characterizes the radial flow. Equations (2) and (4) transform to

$$\eta r^2\frac{d^2v_\phi}{dr^2} + (\eta - c)r\frac{dv_\phi}{dr} - (\eta + c)v_\phi = 0. \tag{5}$$

TABLE I. Variables and parameters.

Variable or parameter	Defining equation(s)	Description
$r_2 > r_1$	(6)	radii of the coaxial cylinders
$x = r/r_2$[a]	(7)	dimensionless radial distance
$x_0 = r_1/r_2$[a]	(28)	dimensionless ratio of the radii
v_ϕ	(1) and (2)	angular velocity
$v_2 = v_\phi(r_2)$, $v_1 = v_\phi(r_1)$	(6)	angular velocities of the coaxial cylinders
v_r	(1) and (2)	radial velocity
$w = x v_r/v_2$[a]	(21)	dimensionless radial velocity
ρ	(1) and (2)	mass density; under normal conditions for air $\rho = 1.2\ \mathrm{kg/m^3}$
p	(1), (2)	pressure
$\rho\epsilon$	(10)	internal energy density
ρs	(39) and (41)	internal entropy density
λ	(10)	heat conductivity; molecular value for air $\lambda_{\mathrm{mol}} = 0.02\ \frac{\mathrm{J}}{\mathrm{ms\,K}}$ (for the turbulent value see Sec. V B)
T	(10)	temperature measured in degrees Kelvin
$\hat{T} = \lambda T/v_2^2\eta$[a]	(21)	dimensionless temperature
$c = \rho v_r r$	(4)	radial flow (c is a constant with this model)
c_p	(4)	isobaric heat capacity; for air $c_p = 10^3\ \frac{\mathrm{J}}{\mathrm{kg\,K}}$
$\hat{c}_p$[a]	(17)	dimensionless isobaric heat capacity; $\hat{c}_p/(\hat{c}_p - 1) = c_p/c_v$ is the ratio of isobaric and isochoric heat capacities
η, ζ	(1) and (2)	viscosities; molecular value for air $\eta_{\mathrm{mol}} = 1.8 \times 10^{-5}\ \frac{\mathrm{kg}}{\mathrm{ms}}$ (for turbulent value see Sec. V A)
$\chi = \eta/\zeta$[a]	(23)	ratio of viscosities
$\alpha = \frac{1-(v_1/v_2)x_0}{1-x_0^{2+\kappa}}$[a]	(9)	weight of the quasisolid vortex in the angular motion
$\kappa = c/\eta$[a]	(22)	$\lvert\kappa\rvert$ is the Reynolds number related to the radial flow
$b = cc_p/\lambda$[a]	(22)	$\lvert b\rvert$ is the Péclet number
β[a]	(23) and (11)	$\lvert\beta\rvert$ is the analog of the Reynolds number related to the radial flow of energy
$\mathrm{Pr} = b/\kappa = \eta c_p/\lambda$[a]	(26)	Prandtl number
$\hat{U}$[a]	(34)	stagnation enthalpy

[a]Dimensionless quantity.

This is a homogeneous equation linear in v_ϕ. Its two independent solutions are obtained by putting $v_\phi \propto r^a$ into (5). The latter produces a quadratic equation for a. This equation has two solutions $a = -1$ and $a = 1 + \frac{c}{\eta}$.

We now impose boundary conditions on inner and outer cylinders, respectively,

$$v_1 \equiv v_\phi(r_1), \quad v_2 \equiv v_\phi(r_2), \tag{6}$$

where $r_2 > r_1$. Then (5) and (6) are solved as a linear combination of the $a = -1$ and $a = 1 + \frac{c}{\eta}$ solutions of (5):

$$v_\phi(r) = v_2 \hat{v}_\phi(x), \quad x \equiv r/r_2, \tag{7}$$

$$\hat{v}_\phi(x) = [(1-\alpha)x^{-1} + \alpha x^{1+\kappa}], \tag{8}$$

$$\kappa \equiv \frac{c}{\eta}, \quad \alpha \equiv \frac{1 - (v_1 r_1)/(v_2 r_2)}{1 - (r_1/r_2)^{2+\kappa}}, \tag{9}$$

where we introduced the dimensionless coordinate x (see Table I). Equation (8) is a weighted sum of two contributions: a potential vortex $1/x$ and a quasisolid vortex x^{1+k}. The weight α can hold both $\alpha > 1$ and $\alpha < 0$.

B. Energy equation

The fluid energy equation reads [29]

$$\partial_t\left(\frac{\rho\vec{v}^2}{2}+\rho\varepsilon\right)+\vec{\nabla}\left[\rho\vec{v}\left(\frac{\vec{v}^2}{2}+\varepsilon\right)+p\vec{v}+\vec{\mu}-\lambda\vec{\nabla}T\right]=0, \tag{10}$$

where $\frac{\rho\vec{v}^2}{2}+\rho\varepsilon$ is the energy density (kinetic energy plus internal energy), $\rho\vec{v}(\frac{\vec{v}^2}{2}+\varepsilon)$ is the advective energy flux, $p\vec{v}$ is the pressure-driven energy flux, T is absolute temperature (measured in degrees Kelvin), $\vec{\nabla}(\lambda\vec{\nabla}T)$ is the heat flux with heat conductivity λ (we assume that λ does not depend on p, ρ, and T), $\mu_k=-\sum_j v_j\sigma_{jk}$ is the energy flow due to viscosity, and σ_{jk} is the stress tensor [29]. With the assumptions and in the stationary regime the energy flux is c_e/r, where c_e is a constant [cf. (4)]:

$$c_e = cE - rv_r\sigma_{rr} - rv_\phi\sigma_{r\phi} - \lambda r\frac{dT}{dr}, \tag{11}$$

$$E=\frac{v_r^2+v_\phi^2}{2}+\varepsilon+\frac{p}{\rho}, \tag{12}$$

$$\sigma_{rr}=2\eta\frac{dv_r}{dr}+\left(\zeta-\frac{2\eta}{3}\right)\frac{1}{r}\frac{d(rv_r)}{dr}, \tag{13}$$

$$\sigma_{r\phi}=\eta\left(\frac{dv_\phi}{dr}-\frac{v_\phi}{r}\right). \tag{14}$$

Here E is the full energy (kinetic plus internal plus potential) per unit of mass, $-\lambda\frac{dT}{dr}$ is the heat flux due to the radial temperature gradient, σ_{rr} and $\sigma_{r\phi}$ are the components of the stress tensor [29], and $v_r\sigma_{rr}$ ($v_\phi\sigma_{r\phi}$) is the rate of radial (angular) work done by viscous forces. Equations (11)–(14) express the first law for the radial flow. Equations (1) and (11) become closed after specifying the thermodynamic state equation; we choose it by assuming that the fluid holds the ideal gas laws (see Appendix A):

$$p=R\rho T/\mu, \tag{15}$$

$$(\rho\varepsilon+p)/\rho=c_pT, \tag{16}$$

$$c_p=\hat{c}_pR/\mu, \tag{17}$$

where $c_p>0$ is the (constant) heat capacity at fixed pressure, $\hat{c}_p$ is a dimensionless number of order 1 (e.g., $\hat{c}_p\approx 3.5$ for air) (see Table I), $R=8.314$ J/K is the gas constant, and μ is the molar mass (29 g for air).

C. Dimensionless parameters and variables

Employing (13)–(17) in (11) and Eqs. (15) and (16) in (1), we end up with the following dimensionless form of (11) and (1), respectively:

$$\left(\frac{\kappa}{2}+1\right)\hat{v}_\phi^2-x\hat{v}_\phi\hat{v}_\phi'+b\hat{T}-x\hat{T}'-\beta+\left(\frac{\kappa}{2}+2\right)\frac{w^2}{x^2}-\left(\chi+\frac{4}{3}\right)\frac{ww'}{x}=0, \tag{18}$$

$$\left(\chi+\frac{4}{3}\right)w''-\left(\kappa+\chi+\frac{4}{3}\right)\frac{w'}{x}+\frac{\kappa w}{x^2}+\frac{\kappa\hat{v}_\phi^2}{w}-\frac{bx}{\hat{c}_p}(\hat{T}/w)'=0, \tag{19}$$

where $x = \frac{r}{r_2}$ [cf. (7) and (9)], a prime means $\frac{d}{dx}$, e.g.,

$$\hat{v}'_\phi = \frac{d\hat{v}_\phi}{dx}, \tag{20}$$

and we have introduced (cf. Table I)

$$\hat{T} = \frac{\lambda}{v_2^2\eta}T, \quad w = \frac{xv_r}{v_2}, \tag{21}$$

$$b = \frac{cc_p}{\lambda}, \quad \kappa = \frac{c}{\eta}, \tag{22}$$

$$\chi = \frac{\zeta}{\eta}, \quad \beta = \frac{c_e}{\eta v_2^2}. \tag{23}$$

Here $|\kappa|$ is the Reynolds number related to the radial flow, while b/κ is the Prandtl number. These and other dimensional and dimensionless parameters of the systems are discussed in Table I. The angular Mach number Ma of the outer cylinder reads, via the above parameters,

$$\mathrm{Ma} = \sqrt{\frac{(\hat{c}_p - 1)\kappa}{b\hat{T}}} = \frac{|v_2|}{v_{\mathrm{sound}}}, \tag{24}$$

where $v_{\mathrm{sound}} = \sqrt{\frac{c_pT}{\hat{c}_p - 1}} = \sqrt{\frac{\hat{c}_p}{\hat{c}_p - 1}\frac{p}{\rho}}$ is the speed of sound for the ideal gas [see (15) and [29]]. The constant β in (18) can be related to $\hat{T}'(1)$ via $\hat{v}'_\phi(1)$ [see (8)]:

$$\hat{T}'(1) = -\beta + b\hat{T}(1) + \left(2 + \frac{\kappa}{2}\right)w^2(1) - \left(\chi + \frac{4}{3}\right)w(1)w'(1) - \alpha(2+\kappa) + 2 + \frac{\kappa}{2}. \tag{25}$$

D. Scaling of temperature

The scaling over v_2 employed in (21) and in (7) does have a physical meaning, since below we show that cooling (i.e., temperature decrease) relates to the angular motion of the cylinders. The choice of the dimensionless temperature $\hat{T}$ is also a reasonable one because, using typical values of experiments [4,27], we find $\hat{T} \sim 1$. Indeed, using (21) we obtain

$$T(r_2) = \hat{T}(1)v_{\mathrm{sound}}^2 \mathrm{Pr}\,\mathrm{Ma}/c_p, \tag{26}$$

where v_{sound} is the sound velocity and $\mathrm{Pr} \equiv \eta c_p/\lambda$ and $\mathrm{Ma} = v_\phi(r_2)/v_{\mathrm{sound}}$ are the Prandtl and Mach numbers, respectively [cf. (24)]. Recall that $\hat{T}(1) = \hat{T}(x = 1)$, where $x = r/r_2 \leqslant 1$ is the dimensionless length. For air we take, in (26), $c_p = 10^3$ J/(kg K) and $v_{\mathrm{sound}} = 3.31 \times 10^2$ m/s. In vortex cooling experiments, the input air has $\mathrm{Ma} \sim 1$ [4,5]. Also $\mathrm{Pr} \sim 1$ holds for air.[3] For an inward flow $c < 0$, the input temperature is $T(r_2)$. We get for it

$$T(r_2) \simeq \hat{T}(1) \times 100. \tag{27}$$

Thus room temperature $T(r_2) \simeq 300$ K means $\hat{T}(1) \simeq 3$.

However, the above scaling of the dimensionless temperature $\hat{T}$ is not applicable for $v_2 \to 0$. Then we should change $v_2 \to v_1$ in (21) and (23) and take instead of (7)

$$v_\phi(r) = v_1\hat{v}_\phi(x), \quad \hat{v}_\phi(x) = \frac{x^{-1} - x^{1+\kappa}}{x_0^{-1} - x_0^{1+\kappa}}, \quad x_0 = \frac{r_1}{r_2}. \tag{28}$$

[3]This relation holds for both the laminar regime and the fully developed turbulence regime [29,41]. For the former (latter) we employ molecular (turbulent) values of heat conductivity and viscosity (see Sec. V).

E. First law

Using (21)–(23), the energy balance (11) can be written in terms of dimensionless local rates of energy $\hat{E}$, radial work $\hat{W}_r$, angular work $\hat{W}_\phi$, and heat $\hat{Q}$:

$$\hat{E}(x) = \frac{c}{\eta v_2^2}\left[\frac{v_r^2(r)+v_\phi^2(r)}{2} + c_p T(r)\right] = b\hat{T} + \frac{\kappa}{2}\left(\hat{v}_\phi^2 + \frac{w^2}{x^2}\right), \tag{29}$$

$$\hat{W}_\phi(x) = -\frac{r}{\eta v_2^2} v_\phi(r)\sigma_{r\phi}(r) = \hat{v}_\phi(x)[\hat{v}_\phi(x) - x\hat{v}_\phi'(x)], \tag{30}$$

$$\hat{W}_r(x) = -\frac{r}{\eta v_2^2} v_r(r)\sigma_{rr}(r) = \frac{2w^2}{x^2} - \left(\chi + \frac{4}{3}\right)\frac{ww'}{x}, \tag{31}$$

$$\hat{Q}(x) = -\frac{\lambda r}{\eta v_2^2} T'(r_1) = -x\hat{T}'(x), \tag{32}$$

where we employed (21)–(23) and (6)–(9). The first law reads, from (11),

$$\Delta\hat{E} + \Delta\hat{W}_r + \Delta\hat{W}_\phi + \Delta\hat{Q} = 0, \tag{33}$$

where $\Delta\hat{E} \equiv \hat{E}(1) - \hat{E}(\frac{r_1}{r_2})$, etc. Note that $\Delta(\hat{W}_r + \hat{W}_\phi) > 0$ means that the system does work on the external sources that immerse the fluid into the system and rotate the cylinders, i.e., the work is extracted.[4] We stress that this model of cooling is not completely autonomous, since it contains moving boundaries. The condition $\Delta\hat{W}_r + \Delta\hat{W}_\phi \geqslant 0$ means that cooling (if it is shown to exist) is not due to external forces that move boundaries. Let us also give the dimensionless form of the stagnation enthalpy

$$\hat{U} = \frac{1}{v_2^2}\left(\frac{\vec{v}^2}{2} + \frac{p}{\rho} + \varepsilon\right) = \frac{\hat{v}_\phi^2}{2} + \frac{w^2}{2x^2} + \frac{b\hat{T}}{\kappa}, \tag{34}$$

which differs from (29) by the factor c/η only.

F. Angular work

The work (30) done by rotating cylinders can be calculated in a closed form from (7), (9), and (14):

$$\Delta\hat{W}_\phi = 2(1-\alpha) - \kappa\alpha - \left[\frac{1-\alpha}{x_0} + \alpha x_0^{1+\kappa}\right]\left[\frac{2(1-\alpha)}{x_0} - \alpha\kappa x_0^{1+\kappa}\right], \quad x_0 \equiv \frac{r_1}{r_2}. \tag{35}$$

Now radially outward flow means $\kappa \geqslant 0$ or $c \geqslant 0$ [see (23)]. For this case we checked numerically that $\Delta W_\phi \leqslant 0$, i.e., the cylinders always invest work. In particular, $\Delta\hat{W}_\phi = 2(1-\alpha)^2(1-x_0^{-2}) < 0$ for $\kappa = 0$. For inward flow $\kappa < 0$ there are situations, where $\Delta W_\phi > 0$, i.e., the work is extracted. Note from (7) and (8) that $\kappa < 0$ means that the angular velocity v_ϕ/r is a decreasing function of r.

G. Cooling efficiency

Any cooling process that is due to a pressure gradient can be usefully compared with the thermodynamic entropy-conserving (adiabatic) process, where the same pressure is employed for cooling. Let $(p_{\text{in}}, T_{\text{in}})$ and $(p_{\text{out}}, T_{\text{out}})$ be, respectively, the input and output pressure and temperature;

---

[4]Note from (10) that the integral $\int_{\partial V} d\vec{s}\,\vec{\mu}$ over a closed surface ∂V is the work done by viscosity forces on the substance enclosed in ∂V. The sign of the work is determined as follows: With the normal vector $\vec{s}$ of ∂V pointing outside, the integral contributes to $-\partial_t \int_{\mathcal{V}} dV(\frac{\rho\vec{v}^2}{2} + \rho\varepsilon)$ [see (10)]. Hence a positive $\int_{\partial V} d\vec{s}\,\vec{\mu}$ means that the fluid in $\mathcal{V}$ does work on external sources.

cooling $T_{\rm out} < T_{\rm in}$ is achieved due to $p_{\rm out} < p_{\rm in}$. For the considered ideal-gas model, the lowest temperature $T_{\rm out,ad}$ reached adiabatically reads (see Appendix A)

$$\frac{T_{\rm out,ad}}{T_{\rm in}} = \left(\frac{p_{\rm out}}{p_{\rm in}}\right)^{1/\hat{c}_p}, \tag{36}$$

where $\hat{c}_p$ is defined in (16) (see also Table I). Hence one defines the cooling efficiency [42]

$$\xi = T_{\rm out,ad}/T_{\rm out}, \tag{37}$$

which has the standard meaning of efficiency (result over effort), since the achieved result of cooling is related to $1/T_{\rm out}$. The pressure difference is a resource and it is quantified by $1/T_{\rm out,ad}$, hence the definition (37).[5]

When quantifying cooling, the Hilsch efficiency is sometimes employed [2,4]:

$$\xi_{\rm H} = \frac{T_{\rm in} - T_{\rm out}}{T_{\rm in} - T_{\rm out,ad}}. \tag{38}$$

The meaning of $\xi_{\rm H}$ differs from that of ξ, because $\xi_{\rm H}$ directly accounts for the input temperature $T_{\rm in}$; however, they are related. As shown by (37), for $T_{\rm in} - T_{\rm out,ad} > 0$ (a natural condition for cooling), $\xi < 1$ ($\xi > 1$) implies $\xi_{\rm H} < 1$ ($\xi_{\rm H} > 1$). However, $\xi_{\rm H}$ is less fundamental than ξ, since it does not appear directly in the efficiency bound imposed by the second law. We discuss this bound now.

H. Second law bound for cooling efficiency

The entropy balance of the fluid reads [29]

$$\partial_t(\rho s) = -\vec{\nabla}\left[s\rho\vec{v} - \frac{\lambda}{T}\vec{\nabla}T\right] + s_{\rm prod}, \tag{39}$$

where ρs is the entropy density and $s\rho\vec{v}$ and $-\frac{\lambda}{T}\vec{\nabla}T$ are, respectively, advective and thermal entropy flux. The entropy production $s_{\rm prod} > 0$ is positive due to viscosity and heat conduction.[6] In the stationary situation $\partial_t(\rho s) = 0$ and (39) reads

$$\frac{d}{dr}\left(cs - \frac{\lambda r}{T}\frac{dT}{dr}\right) = r s_{\rm prod}, \tag{40}$$

where we used (4). The ideal-gas entropy is (cf. Appendix A)

$$s = c_p\left(-\frac{1}{\hat{c}_p}\ln[p] + \ln[T] - \ln\left[\frac{\mu}{R}\right]\right), \tag{41}$$

where we employed (15)–(17).

We consider two particular cases of the adiabatic process (36):

$$r_{\rm in} = r_2, \quad r_{\rm out} = r_1, \quad c < 0, \tag{42}$$

$$r_{\rm in} = r_1, \quad r_{\rm out} = r_2, \quad c > 0. \tag{43}$$

Now (37), (40), (42), and (43) imply

$$s(r_2) - s(r_1) = \mathrm{sgn}[-c]c_p \ln[\xi]. \tag{44}$$

---

[5]Equation (37) is different from the coefficient of performance (COP) of refrigerators, which is defined via the ratio of the heat transferred in refrigeration over the external work performed to achieve this transfer. We do not need the COP, since in our setups the cooling is not achieved due to external work.

[6]The entropy production reads [29] $s_{\rm prod} = \frac{\eta}{2T}[\frac{\partial v_j}{\partial x_k} + \frac{\partial v_k}{\partial x_j} - \frac{2\delta_{jk}}{3}\vec{\nabla}\vec{v}]^2 + \frac{\zeta}{T}[\vec{\nabla}\vec{v}]^2 + \frac{\lambda[\vec{\nabla}T]^2}{T^2} > 0$.

Integrating (40) over r for $r_1 < r < r_2$, using $s_{\rm prod} > 0$, (41), (36), and (44), we get from (42) and (43) an upper bound for the efficiency (37) that applies to both (42) and (43):

$$|b| \ln[\xi] \leqslant \frac{r_1}{T(r_1)} \frac{dT(r_1)}{dr} - \frac{r_2}{T(r_2)} \frac{dT(r_2)}{dr}, \tag{45}$$

where $|b|$ is the Péclet number [see (22) and Table I]. The right-hand side of (45) is nonzero due to heat conductivity. Hence, if the heat conduction is neglected (i.e., $\lambda = 0$) the cooling efficiency holds $\xi < 1$ [see (45)]. We stress again that the inequality in (45) is due to positivity of the entropy production: $s_{\rm prod} > 0$.

III. BOUNDARY CONDITIONS FOR COOLING AND FOR PERMEABLE WALLS

When studying cooling due to a confined gasodynamic flow one should exclude physically uninteresting cases, where the fluid is cooled due to cold thermal baths attached to boundaries or due to external work done by external forces. Cooling demands that the temperature of the (radially) incoming fluid is larger than the temperature of the outgoing fluid. If there is a low-temperature boundary bath, the flow should be thermally isolated from it (adiabatic cooling). Whenever the radial flow is absent, thermal isolation is ensured by imposing vanishing heat flux at boundaries, e.g., at the outer boundary

$$\frac{dT(r_2)}{dr} = 0. \tag{46}$$

If there is a flow through boundaries (i.e., permeable or porous walls), (46) does not hold, because there is a heat conductivity due to the fluid at the boundary.

In addition to known conditions for continuity of temperature and heat flux [29], there is now a specific condition to be satisfied on the adiabatic permeable surface. To understand the origin of this condition, let us "decompose" the macroscopically homogeneous, permeable adiabatic outer surface into holes and solid parts. Recall that (r,ϕ,z) are the cylindrical coordinates. Now for (ϕ,z) elements of holes and a small positive δ, we get that $\frac{d}{dr}T(r_2-\delta;\phi,z)$ stays finite for $\delta \to 0+$. For (ϕ,z) elements of solids, $\frac{d}{dr}T(r_2-\delta;\phi,z)$ goes to zero for $\delta \to 0$. Hence $|\frac{d}{dr}T(r_2-\delta)| > |\frac{d}{dr}T(r_2)|$ after averaging over (ϕ,z), which recovers the macroscopically homogeneous permeable wall. Hence, instead of (46) we obtain the boundary condition

$$\left|\frac{dT(r_2-\delta)}{dr}\right| > \left|\frac{dT(r_2)}{dr}\right|, \quad \mathrm{sgn}\left[\frac{dT(r_2)}{dr}\right]\frac{d^2T(r_2)}{dr^2} < 0, \tag{47}$$

where $\mathrm{sgn}[a] = 1$ if $a \geqslant 0$ and $\mathrm{sgn}[a] = -1$ if $a < 0$, and the second inequality in (47) follows from the first one under $\frac{d}{dr}T(r_2) \neq 0$ and $\delta \to 0+$. Naturally, the first inequality in (47) also holds for $\frac{d}{dr}T(r_2) = 0$, i.e., for an adiabatic wall. Likewise, we have, for the thermally isolated inner wall (for $\delta \to 0+$),

$$\left|\frac{dT(r_1+\delta)}{dr}\right| > \left|\frac{dT(r_1)}{dr}\right|, \quad \mathrm{sgn}\left[\frac{dT(r_1)}{dr}\right]\frac{d^2T(r_1)}{dr^2} > 0. \tag{48}$$

We stress that in the present model (with or without the radial flow) it is trivial to get *arbitrary* low temperatures in between two cylinders. However, generally these temperature profiles do not hold the boundary conditions (47) and (48), i.e., such scenarios of low temperatures do not constitute proper cooling, since they require that low temperatures *preexist* via boundary baths. In particular, Appendix B works out the Couette flow (laminar flow between two infinite rotating cylinders without radial motion), showing that the inhomogeneous temperature profile generated in this flow does not constitute cooling.

Conditions similar to (47) and (48) are deduced for the radial velocity v_r on a partially permeable wall. This is similar to the previous case in that $v_r = 0$ for an impermeable wall [see (46)]. A derivation analogous to that of (47) and (48) produces [cf. (4)]

$$\mathrm{sgn}[c]\frac{dv_r(r_2)}{dr} < 0, \tag{49}$$

$$\mathrm{sgn}[c]\frac{dv_r(r_1)}{dr} > 0 \tag{50}$$

for the outer and inner walls, respectively.

In the present model there are no solutions that support conditions (47) and (48) and conditions (49) and (50) for both inner and outer permeable walls, respectively. Thus we should put them on the wall from which the cold flow is coming (to ensure that low temperatures do not exist before cooling) and leave the other boundary as a control surface, assuming that both the velocity and temperature on this surface are given.

IV. COOLING OF INWARD FLOW

A. Temperature profile for a weak radial flow

Recall from (21) and (9) that κ and $w(x)$ are different dimensionless quantities although both are nonzero due to radial flow. We assume that $w(x)$ and its derivatives are small. Hence factors $(\frac{\kappa}{2}+2)\frac{w^2}{x^2}$ and $(\chi+\frac{4}{3})\frac{ww'}{x}$ are neglected in (18). This can be done provided that x is not very small. However, the influence of the radial flow on the vortex characteristics is not neglected, i.e., $\kappa \neq 0$ [see (6)–(9)]. Now the remainder of (18), i.e., $(\frac{\kappa}{2}+1)\hat{v}_\phi^2 - x\hat{v}_\phi\hat{v}_\phi' + b\hat{T} - x\hat{T}' - \beta = 0$, can be solved explicitly as

$$\hat{T}(x) = g(x) + \frac{\beta}{b} + x^b C, \tag{51}$$

where C is a constant and

$$g(x) \equiv \frac{2x^\kappa\alpha(\alpha-1)}{b-\kappa} - \frac{(1-\alpha)^2(4+\kappa)}{2(2+b)x^2} - \frac{\kappa\alpha^2x^{2+2\kappa}}{2(2-b+2\kappa)}. \tag{52}$$

Now β and C in (51) are conveniently expressed via $\hat{T}(1)$ and $\hat{T}'(1)$ and the temperature profile reads, from (51),

$$\hat{T}(x) - \hat{T}(1) = \frac{x^b-1}{b}[\hat{T}'(1) - g'(1)] + g(x) - g(1). \tag{53}$$

The approximation that led to (53) and (52) is confirmed by solving numerically full equations (18) and (19) (see Figs. 2 and 3).

So far the weak radial flow approximation has amounted to neglecting the radial velocity v_r in the energy equation (18), but retaining it in the angular Navier-Stokes equation (2) [see also (6)–(9)]. If we neglect the radial velocity v_r *also* in the radial Navier-Stokes equation (1) [or equivalently in (19)] we obtain

$$\rho(r)v_\phi^2(r)/r = dp/dr. \tag{54}$$

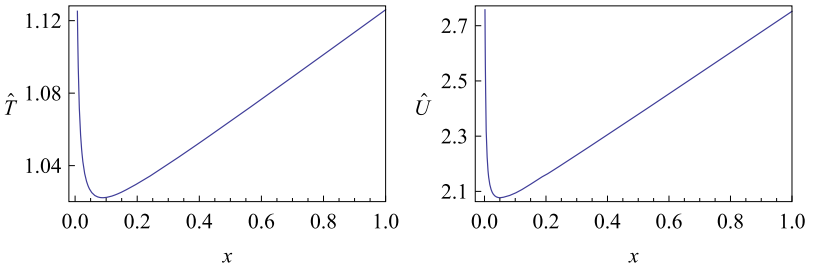

FIG. 2. Isothermal cooling with inward flow ($c < 0$) and a quasisolid vortex (see Sec. IV C). Dimensionless temperature $\hat{T}(x)$ and dimensionless stagnation enthalpy $\hat{U}(x)$ versus dimensionless distance x. Shown on the left (right) is $\hat{T}(x)$ [$\hat{U}(x)$] versus $x = r/r_2$ for $x \in [x_0, 1]$, where $x_0 = 0.007\,347$. The curves are obtained from numerical solution of (18) and (19) for $\alpha = 1$, $\kappa = -0.5$, $b = -1$, $\hat{c}_p = 3.5$, $\beta = -1$ [$\hat{T}'(1) = 0.124$], $\chi = 10$, $\hat{T}(1) = 1.126$, $w(1) = 10^{-4}$, and $w'(1) = 0$. These parameter values are consistent with experiments [27] [see (27), (62), (72), and (74) and the related discussion]. The minimal dimensionless temperature is $\hat{T}_{\min} = \hat{T}(x_{\min}) = 1.0223$ and $x_{\min} = 0.008\,891$. The energy values are $\Delta\hat{E} = -0.246\,99$, $\Delta\hat{W} = 0.482\,28$, $\Delta\widehat{W}_r = -0.014\,05$, $\widehat{Q}(x_0) = -x_0\hat{T}'(x_0) = 0.111\,29$, and $\widehat{Q}(1) = -\hat{T}(1) = -0.124$ [cf. (29)–(33)]. The pressure $p(x)$ is a monotonically increasing function of $x \in [x_0, 1]$ [cf. (55)]. In addition, $\hat{T}_{\rm ad}(x_{\min}) = 0.735\,56$. The Hilsch efficiency is $\xi_{\rm H} = 0.265\,59$ [cf. (38)]. Upon decreasing the initial temperature $x_{\min}$ increases while both the magnitude and quality of cooling decrease, e.g., for $\hat{T}(1) = 1.16$ we get $x_{\min} = 0.505\,97$, $\hat{T}_{\min} = \hat{T}(x_{\min}) = 1.130\,83$, and $\xi_{\rm H} = 0.130\,16$. Further, $w(x)$ [and hence $w(x)/x$] is a monotonically decreasing function of $x \in [x_0, 1]$. Thus condition (50) holds for the inner wall. Condition (49) for the outer wall cannot hold simultaneously with (50); this is why a permeable wall is not imposed at $r = r_2$. The latter is just a control surface within which we describe the flow.

This known equation is solved as[7]

$$\frac{p(x)}{p(1)} = \exp\left[-\frac{\kappa\hat{c}_p}{b}\int_x^1 \frac{dy\,\hat{v}_\phi^2(y)}{y\hat{T}(y)}\right], \tag{55}$$

where $\hat{T}(x)$ and $\hat{v}_\phi(x)$ are given by Eqs. (52) and (53) and Eqs. (7) and (8), respectively. Equation (55) shows that the (dimensionless) pressure is a monotonically increasing function of x.

There are cases, where (52) and (53) are valid, but (54) [and (55)] is not. In Sec. VI we show an important example of this type, where even if $w(x) \to 0$ is imposed in the vicinity of $x = 1$, it does not hold for $x < 1$, because $w(x)$ grows fast.

B. Boundary conditions for inward radial flow

For inward flow $c \leqslant 0$ (hence $b \leqslant 0$ and $\kappa \leqslant 0$) we study cooling scenarios, where the higher-temperature fluid enters into the system through the outer boundary at $x \equiv r/r_2 = 1$. Now for adiabatic boundary conditions, the lower-temperature fluid leaves the system through the inner thermally isolated boundary at $x = x_0 < 1$ [cf. (48)]:

$$\hat{T}(1) > \hat{T}(x_0), \quad \hat{T}''(x_0) > 0. \tag{56}$$

No specific conditions are put at $x = 1$, i.e., it is taken as a control surface.

[7]Let us mention the simplest (but incorrect) argument for the Ranque effect. Setting $\rho(r) = \text{const}$ in (54) and using the ideal gas law $T(r) \propto p(r)$ shows that $T(r)$ is an increasing function of r (i.e., a radial temperature separation is achieved), formally resembling the Ranque effect. The problem with this argument is that it imposes a constant ρ. This may look formally consistent with other equations, but it is incorrect, e.g., because it applies also for $v_r = 0$ (no radial motion whatsoever), while our detailed analysis of this $v_r = 0$ situation shows that no cooling scenarios are possible, because the proper boundary conditions are not satisfied (see Appendix B).

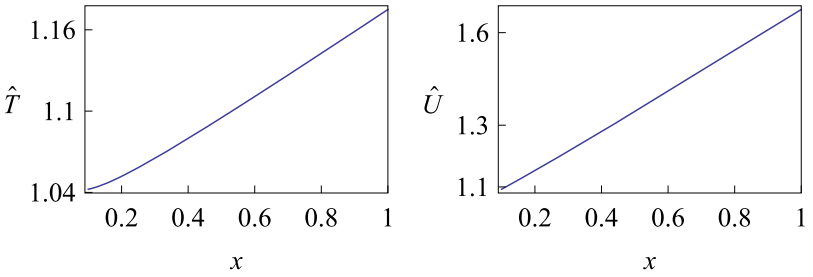

FIG. 3. Adiabatic cooling with inward flow ($c < 0$) and a quasisolid vortex. Dimensionless temperature $\hat{T}(x)$ and dimensionless stagnation enthalpy $\hat{U}(x)$ versus dimensionless distance x. Left (right) figure: $\hat{T}(x)$ [$\hat{U}(x)$] versus $x = r/r_2$ for $x \in [x_0, 1]$, where $x_0 = 0.1$. The curves are obtained from numerical solution of (18), (19) for $\alpha = 1, \kappa = -0.5, b = -0.5, \hat{c}_p = 3.5, \beta = -0.5, \chi = 10$ and $\hat{T}(1) = 1.175, w(1) = 10^{-4}, w'(1) = 0$. The minimal temperature is $\hat{T}(x_0) = 1.04233$. As required for an adiabatic, permeable inner boundary: $\hat{T}''(x_0) = 1.48034$; cf. (47), (48). The energy values are: $\Delta\hat{E} = -0.291278$, $\Delta\hat{W} = 0.44866$, $\hat{Q}(x_0) = -x_0\hat{T}'(x_0) = -0.0051$, $\hat{Q}(1) = -\hat{T}'(1) = -0.1625$; cf. (29)–(33). Efficiency: $\hat{T}_{\rm ad}(x_0) = 0.52012$; see (36), (42). The Hilsch efficiency is $\xi_{\rm H} = 0.2026$. Pressure $p(x)$ and $w(x)$ hold $p'(x) > 0$ and $w'(x) < 0$ for $x \in [x_0, 1]$.

The adiabatic boundary condition (56) relates to the isothermal situation ($x_0 \leqslant x \leqslant 1$)

$$\hat{T}(1) = \hat{T}(x_0) > \hat{T}(x), \tag{57}$$

where $\hat{T}(x)$ assumes a minimum at some $x = x_{\rm min}$. Whenever (57) holds, one can take $x_0 \gtrsim x_{\rm min}$ and this produces an example of (56).

Equation (57) does not refer to a practically useful situation, since no cold fluid really comes out. Nevertheless, it is interesting, since the expected behavior of the temperature is that it is larger inside the fluid, i.e., for $\hat{T}(1) = \hat{T}(x_0)$ we expect $\hat{T}(x) > \hat{T}(1) = \hat{T}(x_0)$ [29]. (The expectation is also confirmed by the example of the Couette flow in Appendix B.) This is because viscosity, which dissipates energy in the bulk of the fluid, generates heat that must be transported out of the boundaries [29]. The expected behavior holds for $c > 0$. However, there are isothermal and adiabatic cooling scenarios for $c < 0$ (see Figs. 2 and 3). We now turn to discuss them.

C. Cooling via a quasisolid vortex

Let us start with a quasisolid vortex in (7) and (8):

$$\alpha = 1 \quad \text{or} \quad v_1/v_2 = (r_1/r_2)^{1+\kappa}. \tag{58}$$

The temperature for this situation reads, from (52) and (53),

$$\hat{T}(x) - \hat{T}(1) = \frac{\left[\hat{T}'(1) + \frac{\kappa}{2}\right][x^b - 1]}{b} + \frac{\kappa(x^b - x^{2+2\kappa})}{2(2 + 2\kappa - b)}. \tag{59}$$

Let us see to what extent (59) can hold the condition (57). Now $\hat{T}'(x_{\rm min}) = 0$ leads to

$$x_{\rm min}^{2-b+2\kappa} = 1 + \frac{(2 - b + 2\kappa)\hat{T}'(1)}{\kappa(1 + \kappa)}, \tag{60}$$

$$\hat{T}''(x_{\rm min}) = -\kappa(1 + \kappa)x_{\rm min}^{2\kappa}. \tag{61}$$

Equation (60) means that $\hat{T}'(x_{\rm min}) = 0$ has only one solution. Since this solution ought to be a minimum [cf. (57)], we have to require $\hat{T}'(1) > 0$, which together with $0 \leqslant x \equiv \frac{r_1}{r_2} \leqslant 1$ leads, from

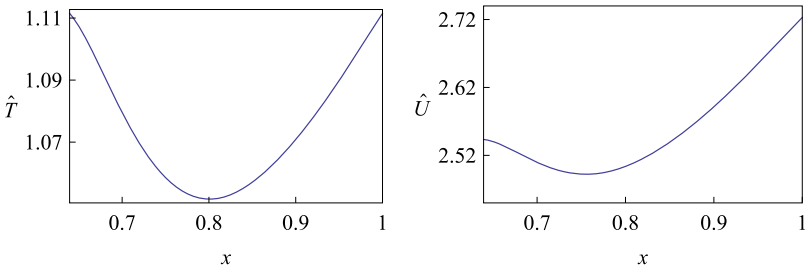

FIG. 4. Isothermal cooling with inward flow and an $\alpha = -0.5$ vortex for dimensionless temperature $\hat{T}(x)$ and dimensionless stagnation enthalpy $\hat{U}(x)$ versus dimensionless distance x. Shown on the left (right) is $\hat{T}(x)$ [$\hat{U}(x)$] versus $x = r/r_2$ for $x \in [x_0, 1]$, where $x_0 = 0.639\,472$. The curves are obtained from numerical solution of (18) and (19) for $\alpha = -0.5, \kappa = -4, b = -5, \hat{c}_p = 3.5, \beta = -7, \chi = 10, \hat{T}(1) = 1.1115, w(1) = 0.01$, and $w'(1) = 0$. The minimal dimensionless temperature is $\hat{T}_{\min} = 1.051\,66$ and it is reached for $x_{\min} = 0.800\,77$. The energy values are $\Delta E = -1.621\,48$, $\Delta W = 2.268\,12$, $\Delta W_r = -0.014\,03$, $\hat{Q}(x_0) = -x_0\hat{T}'(x_0) = 0.204\,143$, and $\hat{Q}(1) = -\hat{T}'(1) = -0.4425$. The pressure $\hat{p}(x)$ [$w(x)$] is a monotonically increasing (resp. decreasing) functions of $x \in [x_0, 1]$. In addition, $\hat{T}_{\rm ad}(x_0) = 0.952\,581$ [see (36) and (42)]. The Hilsch efficiency is $\xi_{\rm H} = 0.376\,542$ [cf. (38)].

(60) and (61), to $\kappa(1+\kappa) < 0$ and $2(1+\kappa) > b$ or, equivalently, to

$$-1 < \kappa < 0, \quad 0 < \hat{T}'(1) < -\frac{\kappa(1+\kappa)}{2(1+\kappa) - b}. \tag{62}$$

Thus, under the conditions (62)and naturally x_0 sufficiently smaller than $x_{\min}$, we get an isothermal cooling scenario (57). Taking $x_0 \gtrsim x_{\min}$, we get instead an example of the adiabatic scenario (56) [cf. the discussion after (57)].

Equations (58) and (62) imply a quasisolid vortex that is frequently observed experimentally. Examples of the above cooling scenario are presented in Figs. 2 and 3 for isothermal and adiabatic scenarios, respectively. Naturally, the cooling takes place in terms of both (thermodynamic) temperature $\hat{T}$ and stagnation enthalpy $\hat{U}$. We will see below that the conditions (58) and (62) are sufficiently representative, i.e., the more general cooling scenarios implied from (53) are close to those predicted by (58) and (62).

D. Magnitude and efficiency of cooling

Both adiabatic and isothermal cooling scenarios lead to relatively weak effects in the sense of

$$\frac{\hat{T}(1) - \hat{T}(x_{\min})}{\min[1, \hat{T}(1)]} \simeq 0.01\text{–}0.1. \tag{63}$$

The cooling magnitude in terms of stagnation enthalpy is larger (see Figs. 2–4).

The efficiency (37) of cooling under the condition (56) is smaller than 1:

$$\xi < 1. \tag{64}$$

Whenever $\frac{d}{dr}T(r_1)$ is sufficiently small, (64) follows directly from the second law bound (45), where $\frac{d}{dr}T(r_2) > 0$ [cf. (42)]. Otherwise, (64) is confirmed numerically (see Figs. 2–4). Hence the Hilsch efficiency (38) also holds $\xi_{\rm H} < 1$, as shown by Figs. 2–4.

For both isothermal and adiabatic cooling scenarios we obtain, from (44) and (64), for the entropy difference,

$$s(r_2) - s(r_1) = c_p \ln[\xi] < 0. \tag{65}$$

Hence the final entropy is always larger than the initial one: $s(r_1) > s(r_2)$.

E. Work and energetics

As shown by (35) and (58), the work done by rotating cylinders is positive under the conditions (62),

$$\Delta\hat{W}_\phi = -\kappa\left(1 - x_0^{2+2\kappa}\right) > 0, \tag{66}$$

which means that the work is extracted. The work $\hat{W}_r$ done by radial external forces is small, but negative (i.e., it is invested), and the overall work is positive (see Figs. 2 and 3). Thus the setup does not demand an external investment of work:[8] Cooling takes place due to the initial pressure larger than the final one, $p(1) > p(x_0)$. In other words, cooling takes place due to the initial potential energy of the fluid.

Under isothermal boundary conditions both thermal baths (at $x = 1$ and $x = x_0$, respectively) provide heat to the system. Using (57) and (58) [and the fact that $w(x)$ is assumed to be small], we get, from (29) and (33),

$$\Delta\hat{E} = \Delta\hat{E}_{\rm kin} = \frac{\kappa}{2}\left[1 - \hat{v}_\phi^2(x_0)\right], \tag{67}$$

which is negative due to (58). Hence we also get cooling in terms of the stagnation enthalpy [see (34) and (29)]. Equations (66) and (67) are consistent with the first law (33), which for the present situation reads $\Delta\hat{E} + \Delta\hat{W} = |\hat{Q}_1| + |\hat{Q}_2|$.

These features hold for other cases of isothermal and adiabatic cooling. Figure 4 shows an isothermal scenario with $\alpha = -0.5$, where $\hat{v}_\phi(x)$ is again a concave increasing function of x. Figure 3 demonstrates an adiabatic cooling scenario that does not reduce to the isothermal case (whenever the latter holds one can obtain an adiabatic scenario by taking $x_0 > x_{\rm min}$).

Let us write, from (11) and (29)–(32),

$$0 = [-\hat{E}(x) + x\hat{T}'(x) - \hat{W}_\phi(x) - \hat{W}_r(x)]'. \tag{68}$$

In (68) we assume that isothermal boundary conditions hold for $c < 0$; hence b and κ are negative. Now $[-\hat{E}(x)]' > 0$ for $x_{\rm min} \lesssim x$, because this means cooling in terms of the stagnation enthalpy. One also has $[x\hat{T}'(x)]' > 0$ for $x_{\rm min} \approx x$. It appears also that $[-\hat{W}_r(x)]' > 0$ has the same sign as $[-\hat{E}(x)]' > 0$. Moreover, it quickly prevails over other factors; this is why for $c < 0$ cooling exists only in the weak radial flow situation, where $\hat{W}_r \to 0$.

Thus, for holding (68) and achieving cooling we need

$$\hat{W}'_\phi(x) > 0, \tag{69}$$

which, using (30), (7), and (8), is equivalent to

$$0 > 4(1-\alpha)^2 + x^{2+\kappa}\alpha(1-\alpha)\kappa(\kappa-2) + 2x^{4+2\kappa}\alpha^2\kappa(\kappa+1). \tag{70}$$

Hence the validity of (69) (at least for certain values of x), i.e., the positivity of work, is a necessary condition for both isothermal and adiabatic cooling in the regime $c < 0$. This condition was obtained in [26], but its necessary character was not properly stressed, in particular, because the heat conductivity and boundary conditions necessary for cooling were neglected. In particular, (69) can lead to mistakes if it is taken as a sufficient condition for cooling.

---

[8]We mention another scenario of cooling, which is realized for the inward flow and the potential vortex $\hat{v}_\phi(x) = 1/x$ [see (8) with $\alpha = 0$]. This scenario is less interesting, since it is driven by external investment of work [$W'_\phi < 0$, as seen from (69) and (70)], while its efficiency and magnitude hold the same constraints (64) and (63). An interesting point of this scenario is that it is accompanied by the kinetic energy that increases in the direction of the flow: $[\frac{|\kappa|}{2}\hat{v}_\phi^2 + |b|\hat{T}(x)]' \leqslant 0$ in (68). Appendix D studies details of this scenario.

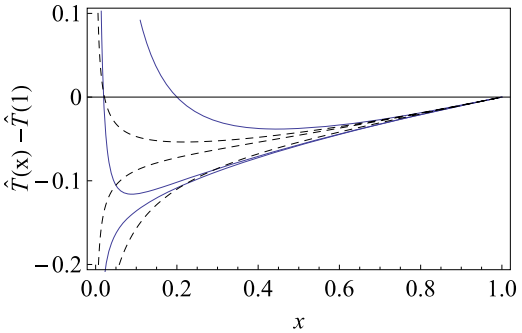

FIG. 5. Dependence of the dimensionless temperature $\hat{T}(x)$ profiles [see (53)] on the radial Reynolds number, where the Prandtl number $\mathrm{Pr} = b/\kappa = 2$ is fixed, the quasisolid vortex condition $\alpha = 1$ is obeyed [see (58)], and $\hat{T}'(1) = 0.1$. Solid blue curves show, from top to bottom, $\kappa = -0.5$, -0.72, and -0.725. The top curve holds condition (56) for all x_0, the middle one holds condition (56) for $x_0 < 0.21$, and the bottom curve (with $\kappa = -0.725$) is void of physical meaning, since neither the adiabatic boundary condition (56) nor the isothermal condition (57) is satisfied for it. Dashed black curves show, from top to bottom, $\kappa = -0.3$, -0.25, and -0.15. For the middle curve the adiabatic boundary condition (56) holds for $x_0 > 0.447$. The bottom curve is void of the physical meaning, since neither (56) nor (57) holds.

F. Dependence of temperature profiles on the radial Reynolds number κ

The radial Reynolds number $\kappa = c/\eta$ (see Table I) combines the radial flow c and the viscosity η. Hence it is important to understand how the cooling temperature profiles depend on κ.

Now κ can change, from one fluid to another, due to c and/or due to η. We will focus on the latter scenario, recalling that η can be an effective (eddy or turbulent) viscosity (see Sec. V for details). Anticipating some of the discussion from Sec. V, we recall that the effective viscosity changes together with the effective heat conductivity λ such that the Prandtl number $\mathrm{Pr} = b/\kappa$ is roughly a constant (also in the turbulent regime) [41]. We also assume that the quasisolid condition (58) holds, i.e., the ratio v_1/v_2 changes together with κ so that $\alpha = 1$ is kept fixed. All these conditions are observed in vortex tubes [4,27].

Figure 5 shows temperature profiles (53) for different values of κ. [Recall that the approximate formula (53) is well confirmed numerically.] It can be seen that the cooling effect disappears for both sufficiently small and sufficiently large values of κ, which we recall is negative for the outward flow due to $c < 0$ (see Table I). This is because the boundary condition (56) ceases to hold. The cooling effect is locally maximal before its disappearance (see Fig. 5).

G. Dependence of cooling on the rotation speed

Since the angular (vortical) motion is necessary for the above cooling scenarios, we turn to studying in detail the dependence of cooling temperature profiles on the rotation speeds v_1 and v_2 of cylinders. It is natural to assume that these variables change by keeping the ratio v_1/v_2 fixed. Now α is a fixed parameter as well [see (9)] and hence we stay within the quasisolid vortex regime. This is useful, because this regime is observed experimentally for a broad range of experimental parameters [4,27].

Since now v_2 is a variable we need to redefine $\hat{T}$ given by (21) (see also Table I). Instead of $\hat{T}$, we employ $\hat{T}_0 = \frac{v_2^2}{v_{2,0}^2}\hat{T} = \frac{\lambda}{v_{2,0}^2\eta}T$, which equals $\hat{T}$ evaluated at some fixed reference value $v_{2,0}$ of the velocity v_2, i.e., $\hat{T}_0$ does not already have a parametric dependence on v_2. Now we get, instead of (53),

$$\hat{T}_0(x) - \hat{T}_0(1) = \frac{x^b - 1}{b}[\hat{T}_0'(1) - \epsilon g'(1)] + \epsilon[g(x) - g(1)], \quad \epsilon \equiv v_2^2/v_{2,0}^2, \tag{71}$$

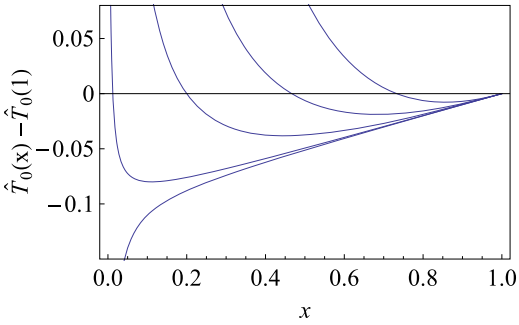

FIG. 6. Dependence of temperature profiles $\hat{T}_0(x) - \hat{T}_0(1)$ on the rotation speed according to (71). A larger ϵ means a bigger deviation of v_2 from its reference values. From bottom to top, $\epsilon = 0.78$ [no cooling is present, since neither (56) nor (57) holds], 0.81, 1, 1.5, and 3. The top four curves demonstrate cooling. For other parameters we set (cf. Figs. 2 and 3) $\hat{T}_0'(1) = 0.1$, $\alpha = 1$, $b = -1$, and $\kappa = -0.5$.

where $g(x)$ is still defined by (52), i.e., it does not have any parametric dependence on v_2 or on ϵ. According to (71), a larger ϵ means a bigger deviation of v_2 from its reference values.

Figure 6 shows temperature profiles (71) for different values of ϵ and for parameters given by (58) and (62). For given values of parameters, there is a value of v_2 where the cooling effect is maximal, i.e., the lowest temperature is reached. For the parameters of Fig. 6 this critical value is found from $\epsilon = 0.8$. When v_2 decreases from this critical value, the cooling effect ceases to exist, since the cooling boundary conditions, as given by (56) or (57), cannot hold anymore, i.e., the curve in Fig. 6 that corresponds to $\epsilon = 0.78$ is void of physical meaning. When v_2 increases from the critical value, the magnitude of vortex cooling, as measured by the lowest temperature reached, monotonically decreases. In particular, for a larger ϵ, we need to take a larger $x_0 = r_1/r_2$ (i.e., $x_0 \to 1$) to achieve cooling (see Fig. 6).

V. RELATION TO EXPERIMENTS

A. Effective viscosity

The actual flow in vortex tubes is highly turbulent [4]. Hence, if one uses hydrodynamic equations (in particular, Navier-Stokes equations) with constant values of viscosities η and ζ and heat conductivity λ, it is at very least necessary to employ there effective (i.e., turbulent or nonmolecular) estimates for these parameters [29,41].

Taking into account that the considered flow is confined and inhomogeneous (i.e., there are radial and angular flows), we choose to estimate the turbulent viscosity η via the Nusselt's formula [43], which was originally proposed for estimating the turbulent viscosity in pipes. Reference [41] found that this formula applies for describing compressible turbulence in a sufficiently wide range of Reynolds numbers. The formula reads [41,43]

$$\eta = 0.15\eta_{\rm mol}[\rho v_\phi l/\eta_{\rm mol}]^{3/4}, \tag{72}$$

where v_ϕ is the characteristic value of the angular velocity, l is the characteristic length, and $\eta_{\rm mol}$ is the molecular viscosity, $\eta_{\rm mol} = 1.8 \times 10^{-5}$ kg/ms for the air. Also, taking in (72) typical experimental parameters for vortex tubes [27], $\rho = 1.2$ kg/m^3, $v_\phi \simeq v_{\rm sound} = 331$ m/s, and $l = 0.1$ m, we get (in kg/ms)

$$\eta \sim 0.085, \tag{73}$$

which is several orders of magnitude larger than $\eta_{\rm mol}$. The estimate (73) roughly coincides with an estimate given in [22] via the mixing-length formula [41] $\eta = \rho\ell^2 \frac{dv_\phi}{dr}$, where $\ell = \beta \frac{dv_\phi}{dr} / \frac{d^2 v_\phi}{dr^2}$ is the

mixing length and β is a suitable numerical constant. It is this specific form of the mixing-length formula that can apply to compressible turbulence [41].

B. Comparison with experiment

Let us recall that the present model omits several physical factors that are met in realistic vortex tubes (see Sec. I for a discussion of basic setups for vortex tubes). In particular, the axial motion is neglected and the fluid is removed radially (in contrast to axial removal in vortex tubes). Hence the model setup has not two, but one output temperature and the whole outgoing fluid is cooled (in contrast to the standard Ranque tube, which has two output flows and achieves temperature separation [4]).

Taking into account (27), the magnitude of cooling is predicted from (63) to be around 10 K. Note that best vortex tubes provide (starting from 300 K) a larger cooling of order 70–80 K [2–4]. Though such a stronger effect is lacking in the present model, we recall that in those cases only a part (e.g., ∼20% according to [2]) of the overall flow is strongly cooled and the remaining part is heated up. In the present model the whole outgoing fluid is cooled.

The Hilsch efficiency ξ_{H} of cooling obtained in the present model is of order 0.1–0.4 (see Figs. 2–4). It also agrees with experiments, though not for the most efficient vortex tubes, where ξ_{H} can be as high 0.6–0.7 [2,4].

The magnitude of the radial flow over the angular flow, expressed by

$$w(1) = 10^{-3}\text{–}10^{-4}, \tag{74}$$

also agrees with experimental measurements [4,5], though it is to be stressed that these measurements were carried out for sufficiently long vortex tubes, where the axial velocities (neglected altogether in the present model) are definitely larger than the radial velocities. The quasisolid vortex (58) for $\hat{v}_\phi(x)$ is also seen experimentally, though the experimental results also indicate that for $x \sim 1$, $\hat{v}_\phi(x)$ starts to decay, i.e., the quasisolid vortex $\hat{v}_\phi(x) \sim x^{1+\kappa}$ (for our model we took $\kappa \sim -0.5$) changes towards the potential vortex $\hat{v}_\phi(x) \sim x^{-1}$ [4,5]. This change of $\hat{v}_\phi(x)$ is given much importance in certain theories of vortex cooling [3,4], but is not present here.

The input density is estimated from (4) and (21):

$$\rho(r_2) = \frac{|\kappa|\eta}{w(1) r_2 v_\phi(r_2)}. \tag{75}$$

Estimating $r_2 \simeq 0.1$ m (a reasonable value for the outer radius of a vortex tube), $v_\phi(r_2) \simeq v_{\mathrm{sound}}$, and η for air as $\eta \simeq 0.085$ kg/ms [see (73)], we end up with $\rho(r_2) \simeq \frac{10^{-3}}{w(1)}$ kg/ms in (75). Estimating from the present model $w(1) \simeq 10^{-4}$ (and recalling $p = R\rho T/\mu$), we get that the input pressure is a few times larger than the atmospheric pressure [1].

Altogether, given the limitations of the present model and complications of the flow in real vortex tubes, one can say that the model is in fair qualitative agreement with experiments, though it is far from predicting (and explaining) the features of the best vortex tubes, those providing the largest efficiency or the largest magnitude of cooling. Savino and Ragsdal presented a simplified setup of vortex cooling effect [27] that in several respects is similar to the present model. They studied two short (compared to the diameters) concentric cylinders; the length to diameter ratio was 0.1 and 0.5 for two different samples. (For traditional Ranque-Hilsch tubes the length to diameter ratio is 20–50.) The rotating air enters radially from the whole outer permeable cylinder and leaves through the inner (smaller) cylinder. Rotational flow was created via the outer cylinder with Mach number ≃0.2. The velocity of this flow was much larger than that of the radial flow. The authors found a cooling effect in terms of the radial variation of the stagnation enthalpy[9] (no data on thermodynamic

[9]Recall that (due to Bernoulli's theorem) cooling in terms of the stagnation, enthalpy cannot be explained via adiabatic fluid dynamics.

temperature or velocities were given). The magnitude of this cooling effect is lower than predictions of the present model (cf. the stagnation enthalpy data in Figs. 2 and 3). They confirmed that the radial distribution of the stagnation enthalpy is established already near the end wall of the tube and is not affected by the weak axial flow. In particular, the axial change of the stagnation enthalpy was much smaller than the radial one. (Hence it was legitimate to neglect the axial flow in the model.) They found that the experimental data can be described by (54), where pressure is balanced by the centrifugal force (this equation does not contain the viscosity explicitly). It was observed that the pressure decreases monotonically with the radius, as confirmed by (55) of the present model.

VI. COOLING OF OUTWARD FLOW

A. Conditions for cooling

Now we assume that $c > 0$ (i.e., $\kappa > 0$ and $b > 0$) and the outer boundary of the system is thermally isolated in the sense of (47). Hence, since the outgoing fluid is colder than incoming one, this implies (for $c > 0$) that $\hat{T}'(1) < 0$ and then (47) demands

$$\hat{T}''(1) > 0 \tag{76}$$

at the adiabatic outer boundary. No specific conditions are imposed at the inner boundary $r = r_1$ that can be thus considered as a control surface.

The full expression for $\hat{T}''(1)$ is worked out from (18) and (19) [recall (25)]:

$$\hat{T}''(1) = \frac{b\hat{T}'(1)w'(1)}{\hat{c}_p w(1)} + \left[\frac{b(\hat{c}_p - 1)}{\hat{c}_p} - 1\right]\hat{T}'(1) - \left(\chi + \frac{1}{3}\right)w'(1)^2 - [2w(1) - w'(1)]^2 - [\alpha(2+\kappa) - 2]^2. \tag{77}$$

The first line of (77) contains potentially positive terms, while all the terms in the second line of (77) are nonpositive. Hence (76) demands that the second line of (77) is sufficiently small, e.g., via $w'(1) \to 0$. Likewise, $\hat{T}'(1)$ cannot be very small.

If $w(x)$ and $w'(x)$ are sufficiently small, $\hat{T}(x)$ can be approximately determined from (52) and (53). However, (54) and (55) do not apply anymore, because the (dimensionless) pressure $\hat{p}(x) = \hat{T}(x)/w(x)$ is now a decreasing function of x for $x \in [x_0, 1]$. Thus, $w(x)$ is now essential in (19) and it is important for determining the energetics. The physical reason for this is that the work $\Delta\hat{W}_r$ [see (31)] done by viscous radial forces is relevant, as shown below.

Figure 7 demonstrates the main outward-flow cooling scenario for $\alpha = 1$ [cf. (8)]. The magnitude of cooling is now sizable,

$$[\hat{T}(x_0) - \hat{T}(1)]/\hat{T}(x_0) \geqslant 10. \tag{78}$$

The temperature profile $\hat{T}(x)$ shown in Fig. 7 coincides with that found from (59) and (60), where now $\hat{T}'(1) < 0$ and $x_{\min}$ in (60) should be changed to $x_{\max}$, because this is now the maximum of $\hat{T}(x)$. Then one should take $x_0 > x_{\max}$ so that the temperature decreases for $x_0 < x < 1$.

B. Energetics, entropy, and efficiency

We expectedly have

$$\hat{Q}(x_0) = -x_0\hat{T}'(x_0) > 0, \quad \hat{Q}(1) = -\hat{T}'(1) > 0, \tag{79}$$

i.e., the heat enters from the inner boundary $x = x_0$ and leaves at the outer boundary $x = 1$ [see (48)]. We see numerically that $\hat{Q}_1 \lesssim \hat{Q}_2$ (see Fig. 7). Now $\Delta\hat{W}_\phi < 0$ (rotating cylinders invest work), as we discussed after (30). However, the radial external forces do extract work $\Delta\hat{W}_r > 0$ so much that the total work is extracted (see Figs. 7 and 8):

$$\Delta\hat{W} = \Delta\hat{W}_r + \Delta\hat{W}_\phi > 0. \tag{80}$$

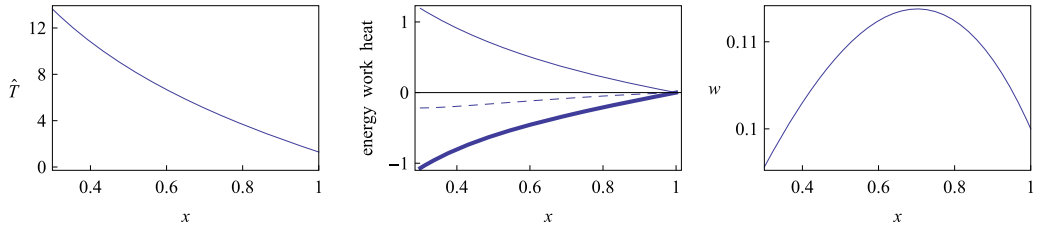

FIG. 7. Adiabatic cooling with weak outward radial flow and quasisolid vortex for dimensionless temperature $\hat{T}(x)$, energy quantities, and dimensionless radial velocity w versus dimensionless distance x (see Table I). Equations (18) and (19) are solved numerically for $\alpha = 1$, $\kappa = 0.1$, $b = 0.1$, $\hat{c}_p = 3.5$, $\beta = 11$ $[\hat{T}'(1) = -10.7867]$, $\chi = 10$, $\hat{T}(1) = 1.295$, $w(1) = 0.1$, and $w'(1) = -0.1$ in the range $x = r/r_2 \in [x_0, 1]$, where $x_0 = 0.3$. Shown on the left is $\hat{T}(x)$ versus $x = r/r_2$ [the dimensionless stagnation enthalpy $\hat{U}(x)$ behaves similarly]. A nearly identical temperature profile is obtained upon solving (18) with $w(x) = w(1)$ and $w'(x) = 0$. Shown in the middle are the dimensionless energy $\hat{E}(x) - \hat{E}(1)$ (solid line), radial work $\hat{W}_r(x) - \hat{W}_r(1)$ (dashed line), and heat $\hat{Q}(x) - \hat{Q}(1)$ (bold line) versus x. Shown on the right is $w(x)$ versus x. The condition (49) holds. It is written as $w(x_0) > x_0 w'(x_0)$ and $w(1) > w'(1)$. The radial velocity proportional to $w(x)/x$ is a monotonically decreasing function of x. The minimal (maximal) dimensionless temperature is $\hat{T}(1) = 1.295$ $[\hat{T}(x_0) = 13.6389]$ and $\hat{T}''(1) = 9.98$. The energy values are $\Delta\hat{E} = -1.1925$, $\Delta\hat{E}_{\rm kin} = 0.041\,88$, $\Delta\hat{W}_r = 0.217\,43$, $\Delta\hat{W} = 0.1245$, $\hat{Q}(x_0) = -x_0\hat{T}'(x_0) = 9.7187$, and $\hat{Q}(1) = -\hat{T}'(1) = 10.885$. The efficiency $\hat{T}_{\rm ad}(1) = 6.8718 > \hat{T}(1) = 1.295$ and the Hilsch efficiency is $\xi_{\rm H} = 1.8241$. The pressure $p(x)$ is a decreasing function of x.

Moreover, the overall kinetic energy [see (29)] also increases, $\Delta\hat{E}_{\rm kin} > 0$ (albeit slightly, as shown in Fig. 7), due to the contribution $\frac{\kappa}{2}(1 - x_0^{2+2\kappa})$ of the vortex.

The most interesting aspect of this cooling scenario is that the cooling efficiency (37) is larger than 1 (see Fig. 7):

$$\xi \geqslant 1, \tag{81}$$

i.e., the adiabatic process provides less cooling, since now the heat transfer from the system is essential [see after (45)]. Together with (81), the Hilsch efficiency (38) is also larger than 1: $\xi_{\rm H} > 1$ (see Fig. 7).

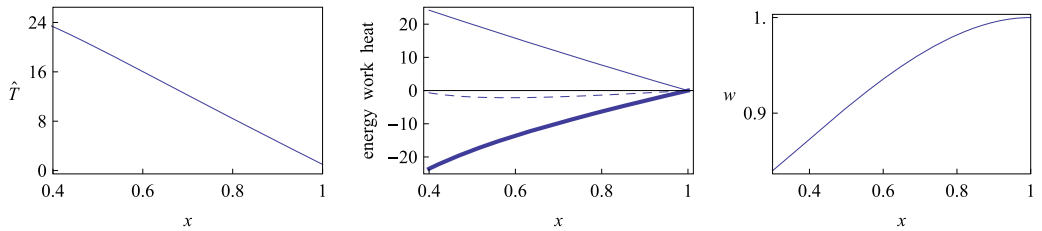

FIG. 8. Adiabatic cooling with outward ($c > 0$) radial flow and without vortex motion ($v_\phi = 0$) for dimensionless temperature $\hat{T}(x)$, energy quantities, and dimensionless radial velocity w versus dimensionless distance x (see Table I). The curves are obtained from numerical solution of (18) and (19) for $\kappa = 1$, $b = 1$, $\hat{c}_p = 3.5$, $\beta = 40$ $[\hat{T}'(1) = -36.5]$, $\chi = 10$, $\hat{T}(1) = 1$, $w(1) = 1$, and $w'(1) = 0$. Shown on the left is $\hat{T}(x)$ versus $x = r/r_2$ for $x \in [x_0, 1]$, where $x_0 = 0.4$ [the dimensionless stagnation enthalpy $\hat{U}(x)$ behaves similarly]. Shown in the middle are the dimensionless energy $\hat{E}(x) - \hat{E}(1)$ (solid line), radial work $\hat{W}_r(x) - \hat{W}_r(1)$ (dashed line), and heat $\hat{Q}(x) - \hat{Q}(1)$ (bold line) versus x. Shown on the right is $w(x)$ versus x. The condition (49) holds (cf. the data for Fig. 7). It also holds that $[w(x)/x]' < 0$. The minimal dimensionless temperatures are $\hat{T}(1) = 1$ and $\hat{T}''(1) = 6.4293$. The energy values are $\Delta\hat{E}_{\rm kin} = -1.8809$, $\Delta\hat{W} = \hat{W}_r = 0.6676$, $\hat{Q}(x_0) = -x_0\hat{T}'(x_0) = 12.9593$, and $\hat{Q}(1) = -\hat{T}'(1) = 36.5$. The efficiency $\hat{T}_{\rm ad}(1) = 9.123\,73 > \hat{T}(1) = 1$ and the Hilsch efficiency is $\xi_{\rm H} = 1.5719$. The pressure $p(x)$ is a decreasing function of x.

Equation (81) is thermodynamically consistent. Recalling (39) and (43), we see that the upper bound (45) amounts to $\frac{x_0\hat{T}'(x_0)}{\hat{T}(x_0)} - \frac{\hat{T}'(1)}{\hat{T}(1)}$. This expression is positive [cf. (79)]. Hence it is possible to have (81) provided that the entropy production is sufficiently small, which appears to be the case, as confirmed numerically. We stress again that $\xi > 1$ is possible due to heat conductivity [cf. the discussion after (45)].

Due to (39) and (81), the entropy entering to the system is larger than the one that leaves it [cf. (65)]:

$$s(r_2) - s(r_1) = c_p \ln[1/\xi]. \tag{82}$$

Thus we get that (without any investment of overall external work) the temperature, stagnation enthalpy, and entropy decrease, while the kinetic energy increases. The outgoing fluid is more ordered, since not only its thermal energy decreases, but also the kinetic energy increases.

C. Physical mechanisms of the effect and cooling without vortical motion

We saw around (68) and (69) that in order to get inward flow cooling it is necessary to have an angular motion with the viscous forces doing work of the proper sign. Here the physical meaning of cooling can be clarified along the same lines. We get, from (18) and (29)–(32),

$$0 = [\hat{E}(x) + \hat{Q}(x) + \hat{W}_r(x) + \hat{W}_\phi(x)]'. \tag{83}$$

Now cooling implies that outgoing fluid has lower energy: $\hat{E}'(x) < 0$. Possible necessary conditions for cooling is provided by the heat conductivity, $\hat{Q}'(x) > 0$, and/or by the work done via radial viscosity, $\hat{W}_r'(x) > 0$. Figures 7 and 8 show that both these conditions hold. The contribution of $\hat{Q}'(x) > 0$ is larger than that of $\hat{W}_r'(x) > 0$.

However, the vortex contribution has the same sign as energy: $\hat{W}_\phi'(x) < 0$ [cf. with (69)]. Hence a similar cooling scenario is also possible without a vortex, i.e., for $\hat{v}_\phi = 0$ in (18) and (19). In fact, eliminating the angular motion almost does not change the temperature profile in Fig. 7. The main difference with the above situation is that the kinetic energy decreases, $\Delta E_{\rm kin} < 0$, since the vortex motion is now absent.

Note that to eliminate the vortex from equations of motion, one should take $v_\phi = 0$ in (18) and (19) and to suppress the last factor $-\alpha(2+\kappa) + 2 + \frac{\kappa}{2}$ in (25) as well as $-[\alpha(2+\kappa) - 2]^2$ in the second line of (77). The definitions (21)–(23) of dimensionless parameters still apply, where now $v_2 = v_{2,0}$ is an arbitrary characteristic velocity (see Sec. IV G). It drops out from (18) and (19).

A simple analytical description of the temperature profile can be obtained from (18) assuming that the change of $w(x)$ can be neglected. [However, note that the change of $w(x)$ within (19) cannot be neglected.] Taking in (18) $\hat{v}_\phi = 0$, $w(x) = w(1)$, and $w'(x) \to 0$, we get

$$\hat{T}(x) - \hat{T}(1) = \gamma\left[1 - \frac{1}{x^2}\right] + [2\gamma - \hat{T}'(1)]\frac{1 - x^b}{b}, \tag{84}$$

$$\gamma \equiv \frac{w(1)^2(4+\kappa)}{2(2+b)}. \tag{85}$$

Now $\hat{T}'(x) = 0$ is solved as $x_{\rm max}^{b+2} = \frac{2\gamma}{2\gamma - \hat{T}'(1)}$. This solution exists only for $\hat{T}'(1) < 0$ (recall that $b > 0$) and it is a maximum of $\hat{T}(x)$. Hence one should take $x_0 > x_{\rm max}$ in order to get a monotonic decrease of temperature $\hat{T}(x)$ from $x = x_0$ until $x = 1$.

One feature of this cooling scenario is that once $w(1)$ (the boundary condition for the outward flow) decreases, the solution of hydrodynamic equations (18) and (19) ceases to exist below a certain critical value of $w(1)$, because now $w(x_0)$ becomes negative. Recall from (4) that a negative $w(x_0)$ for $c > 0$ is not acceptable, since it would mean a negative mass density ρ. Thus, if $w(1)$ is decreased, then c also has to decrease to keep the solution physical.

Generally, the magnitude (78) of the cooling increases upon decreasing the radial flow c, i.e., for $c \to 0$. This can be seen from (84) or from Fig. 8. However, this limit $c \to 0$ is not useful, since it diminishes the cooling power $b[\hat{T}(x_0) - \hat{T}(1)]$.

D. Geometric aspects of the cooling effect

Note that the present cooling scenario (without vortex) is specific for the cylindrical geometry. Its traces are seen in one dimension (plane geometry), but the cooling as such is negligibly weak there (see Appendix C).

To understand the origin of this effect, let us take the situation where all the velocities vanish (hence $c = 0$). Due to the cylindrical geometry, (11) shows that there is still a nontrivial stationary temperatures profile $c_e = -\lambda r T_0'$ that reads, in terms of the dimensionless temperature $\hat{T}$ and dimensionless length $x = r/r_2$ ($x_0 \leqslant x \leqslant 1$),

$$\hat{T}_0(x) - \hat{T}_0(1) = \hat{T}_0'(1) \ln x. \tag{86}$$

Now it should be clear that (86) does not describe as such any cooling effect. Indeed, for $\hat{T}_0'(1) \leqslant 0$ we should put a thermally isolated wall at $x = 1$ (to avoid assuming the existence of even colder temperatures), which leads us to $\hat{T}_0'(1) = 0$ and hence to a constant temperature profile.

However, there is a relation between (86) and the temperature profiles obtained above for $c > 0$ and illustrated in Figs. 7 and 8:

$$\hat{T}_0(x) > \hat{T}(x) \quad \text{if } \hat{T}_0'(1) = \hat{T}'(1) < 0,\ \hat{T}_0(1) = \hat{T}(1), \tag{87}$$

where we note from (86) that $\hat{T}_0''(1) = -\hat{T}_0'(1)$, i.e., for $\hat{T}_0'(1) = \hat{T}'(1) < 0$, $\hat{T}_0''(1)$ agrees with the boundary condition (47) required for cooling. Equation (87), which we verified numerically, shows that the reported cooling effect is the modification of the formal temperature profile (86) to the physical, situation with $c > 0$. In the one-dimensional case (plane geometry) the general zero-velocity temperature profile [the analog of (86)] is just $T_0 = \text{const}$, which explains why the cooling effect is negligible there (see Appendix C).

VII. SUMMARY

We worked out a tractable model for describing gasodynamic cooling. The model extends the standard Couette flow between two coaxial cylinders by adding there a radial flow (hence demanding that cylinders are permeable). Only the radial dependence of relevant quantities is retained and the axial flow is neglected.

The model accounts for viscosity, heat conductivity, and compressibility (see Sec. II). They are *generally* important for gasodynamic cooling and there are at least two reasons for keeping each of them in the description. Viscosity is to be retained, first since we should achieve cooling also in terms of the stagnation enthalpy (as observed experimentally [27]) and second since, due to turbulence, the actual viscosity is much larger than its molecular value. Heat conductivity is to be considered simultaneously with viscosity since the Prandtl number of air is close to 1. It is also important for ensuring boundary conditions of cooling. Compressibility is needed because we need the proper relation between fluid mechanics and thermodynamics and also because the involved angular velocities are sonic.

The emphasis of our study is not so much in describing details of the vortex cooling effect as observed in experimental examples of vortex tubes, but rather in showing how a hydrodynamic model can account for cooling via specific boundary conditions (see Sec. III) and how already the simplest model can provide new (and thermodynamically consistent) predictions for cooling with efficiency larger than 1. We showed that the model predicts a vortex cooling effect for an inward radial flow (see Sec. IV). Though the general cause of cooling is in the pressure gradient that drives the flow, the local cause is related to the work done by viscous forces. The cooling effect comes in two versions, adiabatic and isothermal, that are closely related, but differ from each other by the boundary

conditions. In several ways the obtained cooling effect is similar to what was experimentally seen in Ref. [27] for a short uniflow vortex tube. In accord with experimental results, the model predicts that the efficiency of vortex cooling is generically smaller than 1 (see Sec. II G), though the concrete values for the efficiency and for the magnitude of cooling are lower than what was observed for best vortex tubes.

The model predicts as well a cooling effect that so far has not been observed experimentally (see Sec. VI). This effect is realized for an outward flow and it does not need an angular (vortical) motion. Its cooling efficiency is larger than 1, i.e., for the given gradient of pressure, this cooling is more efficient than the adiabatic (i.e., entropy conserving) thermodynamic process. This cooling effect is consistent with the second law and it is possible due to heat conductivity. It has partly a geometric origin, since it is negligible for the plane geometry.

There is an experimental report on the Hilsch efficiency being larger than 1 for a counterflow tube (where only a part of the air is cooled) [44]. However, this result was not reproducible in [6]. According to the author of Ref. [6], the report concerned externally cooled vortex tubes (cf. our discussion in Sec. III). Hence we conclude by stressing that cooling with an efficiency larger than 1 is an open problem.

APPENDIX A: IDEAL GAS THERMODYNAMICS

We briefly recall ideal-gas formulas as applied in hydrodynamics. Thermodynamic relations of hydrodynamics are written for extensive quantities, which are divided by the overall number N of involved particles and by the mass m of a single particle. Thus the extensive ideal gas entropy

$$S = k_{\rm B} C_v \ln[p] + k_{\rm B} C_p \ln[V/Nm], \tag{A1}$$

where C_v and C_p are heat capacities and V is the volume, becomes

$$s = \frac{S}{Nm} = \frac{k_{\rm B}}{m}\frac{C_v}{N}\ln[p] + \frac{k_{\rm B}}{m}\frac{C_p}{N}\ln[V/Nm] = \frac{k_{\rm B}N_A}{N_A m}\hat{c}_v \ln[p] - \frac{k_{\rm B}N_A}{N_A m}\hat{c}_p \ln[\rho], \tag{A2}$$

where $\rho = Nm/V$ is the mass density, N_A is the Avogadro number, and $\hat{c}_v$ and $\hat{c}_p$ are dimensionless numbers of order 1:

$$\hat{c}_p - \hat{c}_v = 1. \tag{A3}$$

After defining

$$k_{\rm B} N_A = R, \quad N_A m = \mu, \tag{A4}$$

where $R = 8.314$ J/K is the gas constant and μ is the molar mass, (A2) reads

$$s = c_v \ln[p] - c_p \ln[\rho], \tag{A5}$$

$$c_v = (R/\mu)\hat{c}_v, c_p = (R/\mu)\hat{c}_p. \tag{A6}$$

The full entropy S (and similarly other extensive quantities) is obtained as $S = \int_V d^3x\, \rho s$. Noting that the temperature T is measured in degrees Kelvin, the ideal gas equation of state $pV = k_{\rm B} NT$ becomes

$$p = (R/\mu)\rho T. \tag{A7}$$

For purposes of dimensionless analysis, we write (A5) as

$$s = c_p\left(-\frac{1}{\hat{c}_p}\ln[p] + \ln[T] - \ln\left[\frac{\mu}{R}\right]\right). \tag{A8}$$

Equation (A8) implies that if the pressure and temperature adiabatically (i.e., for a constant entropy) change as $p \to p'$ and $T \to T'$, then

$$T'/T = (p'/p)^{1/\hat{c}_p}. \tag{A9}$$

APPENDIX B: VORTEX FLOW WITHOUT RADIAL MOTION (COUETTE FLOW)

Consider the distribution of temperature inside the vortex (7) when the radial motion is absent. This is one of standard problems of hydrodynamics (the Couette flow) and it has been studied in many places (see, e.g., [29,45]). We reconsider this problem here because we want to understand why specifically this situation does not contain any interesting stationary cooling scenario (contrary to remarks given in [45]). For

$$v_r = c = w = \kappa = b = 0, \tag{B1}$$

we get $(\frac{\kappa}{2}+1)\hat{v}_\phi^2 - x\hat{v}_\phi\hat{v}_\phi' + b\hat{T} - x\hat{T}' - \beta = 0$ from (18). This equation integrates and determines temperature inside the vortex ($x \equiv r/r_2$)

$$\hat{T}(x) = \hat{T}(1) - (1-\alpha)^2\left(\frac{1}{x^2} - 1\right) + [\hat{T}'(1) - 2(1-\alpha)^2]\ln x, \quad x_0 \equiv \frac{r_1}{r_2} \leqslant x \leqslant 1, \tag{B2}$$

where we employed (25) and (B1) for expressing β via $\hat{T}'(1)$ and α is given by (9) under $\kappa = 0$:

$$\alpha = \frac{1 - v_1 r_1/v_2 r_2}{1 - (r_1/r_2)^2}. \tag{B3}$$

Note that taking the inner radius r_1 to zero, $r_1 \to 0$, does not lead to anything interesting: In this limit we get $\alpha \to 1$ and (B2) implies $\hat{T}(x) = \hat{T}(1) + \hat{T}'(1)\ln x$, but we have to assume also $\hat{T}'(1) = 0$ to prevent the singularity at $x \to 0$. Then $\hat{T}(x)$ does not depend on x. Hence r_1 should be kept finite.

Interesting (stationary) cooling scenarios are those where the low temperatures created inside the fluid are not due to even lower temperatures imposed on its boundary. In particular, if one of the boundaries is left without thermal isolation, so there is an active thermal bath working at this boundary, then the inside temperature should be lower than the temperature of this bath.

Let us start with the case, where no thermal isolation is imposed for both boundaries. Then $\hat{T}(x)$ should have a local minimum at some $x \in (x_0, 1)$. Equation (B2) shows that there is only one solution $x = x_{\max}$ of $\hat{T}'(x) = 0$:

$$x_{\max} = \sqrt{\frac{2(1-\alpha)^2}{2(1-\alpha)^2 - \hat{T}'(1)}}. \tag{B4}$$

If $0 < x_{\max} < 1$ [for which it is necessary and sufficient that $\hat{T}'(1) < 0$], then $x_{\max}$ is the local maximum (not minimum) of $\hat{T}(x)$. Hence we get no cooling for this case.

Next let us thermally isolate the outer boundary $\hat{T}'(1) = 0$. We get, from (B2),

$$\hat{T}(x) - \hat{T}(1) = -(1-\alpha)^2\left(\frac{1}{x^2} - 1 - \ln\left[\frac{1}{x^2}\right]\right). \tag{B5}$$

Then $\hat{T}(x)$ is a monotonically increasing function of x, i.e., the inside temperature $\hat{T}(x)$ is larger than the (inner) bath temperature $\hat{T}(x_0)$. For a thermally isolated inner boundary $\hat{T}'(x_0) = 0$, $\hat{T}(x)$ is a monotonically decreasing function of x [see (B4)], i.e., again we get no interesting scenarios of cooling. There are no solutions when both boundaries are thermally isolated [see (B2)].

The absence of interesting cooling scenarios is confirmed by looking at the total work produced by external forces that rotate the cylinders. It reads, from (35) (with $\kappa = 0$),

$$\hat{W}_\phi = 2(1-\alpha)^2\left(1 - \frac{1}{x_0^2}\right) < 0. \tag{B6}$$

The negativity of (B6) means that the work is invested externally and dissipated to overcome the viscous forces. This work leaves the system as heat.

Thus three regimes are impossible for the considered Couette flow.

(i) It cannot cool the fluid isothermally, i.e., when both boundaries are kept at the same temperature.

(ii) It cannot cool the fluid adiabatically: No regime exists when one boundary is thermally isolated while another one is subject to a thermal bath and it is necessary to get the fluid colder than the active bath temperature. Hence low temperatures present in the system according to (B2) do not constitute any nontrivial cooling: They are due to the low-temperature bath present at one of boundaries. Put differently, for the Couette flow the active bath is the one with the lower temperature.

The above two conclusions seem to hold rather generally for stationary hydrodynamic systems without mass flow, though we so far did not get a general argument for their validity. At any rate they hold for the (generalized) Couette (sometimes also called Taylor-Dean) flow, where the fluid is subject to azimuthal driving with a volume force $\vec{f}$, where only the ϕ component $f_\phi(r)$ of $\vec{f}$ is nonzero, but it is an arbitrary function of r.

(iii) The Couette flow cannot also function as a heat engine since, irrespectively of the values of $T(r_2)$ and $T(r_1)$, the work is always dissipated [see (B6)].

APPENDIX C: EXAMPLE OF WEAK ADIABATIC COOLING

Consider a one-dimensional flow (from left to right) between two permeable plates separated by distance L. Continuity of mass leads to

$$\rho v = c_1 = \text{const}. \tag{C1}$$

One-dimensional Navier-Stokes and energy equations read, in dimensionless form,

$$\kappa \hat{v}^2(x) + \frac{b}{\hat{c}_p}\hat{T}(x) - \left(\chi + \frac{4}{3}\right)\hat{v}(x)\hat{v}'(x) = \gamma \hat{v}(x), \tag{C2}$$

$$\frac{\kappa}{2}\hat{v}^2(x) + b\hat{T}(x) - \left(\chi + \frac{4}{3}\right)\hat{v}(x)\hat{v}'(x) - \hat{T}' = \beta, \tag{C3}$$

where $0 \leqslant x \leqslant 1$, L is the distance between two plates, β and γ are constants, and we introduced the dimensionless parameters

$$\hat{T} = \frac{\lambda}{v_2^2\eta}T, \quad \hat{v}(x) = \frac{v(x)}{v(L)}, \tag{C4}$$

$$b = \frac{c_1 c_p L}{\lambda}, \quad \kappa = \frac{c_1 L}{\eta}, \tag{C5}$$

$$\chi = \frac{\zeta}{\eta}, \quad \hat{c}_p = c_p(\mu/R). \tag{C6}$$

The constants β and γ can be expressed via, respectively, $\hat{v}'(1)$ and $\hat{T}'(1)$:

$$\gamma = \kappa + \frac{b}{\hat{c}_p}\hat{T}(1) - \left(\chi + \frac{4}{3}\right)\hat{v}'(1), \tag{C7}$$

$$\beta = \frac{1}{2}\kappa + b\hat{T}(1) - \left(\chi + \frac{4}{3}\right)\hat{v}'(1) - \hat{T}'(1). \tag{C8}$$

We obtain, from (C4)–(C7),

$$\hat{T}''(1) = b\hat{T}'(1)\left(1 - \frac{1}{\hat{c}_p}\right) - \left(\chi + \frac{4}{3}\right)\hat{v}'(1)^2 + \frac{b}{\hat{c}_p}\hat{T}(1)\hat{v}'(1). \tag{C9}$$

Let us now look at conditions for adiabatic cooling. Now $c_1 > 0$ (hence $b > 0$ and $\kappa > 0$) and $\hat{v} > 0$ from (C1). Hence we look for

$$\hat{T}(0) > \hat{T}(1), \quad \hat{T}''(1) > 0. \tag{C10}$$

The temperature profiles appear to be monotonic so that the first condition in (C10) can be written as $\hat{T}'(1) < 0$. Then the first and second terms on the right-hand side of (C9) are negative. Hence $\hat{T}''(1) > 0$ can be satisfied only due to sufficiently large $\frac{b}{\hat{c}_p}\hat{T}(1)\hat{v}'(1) > 0$. This implies limitations on $T(1)$ (which cannot be sufficiently small) and on $|\hat{T}'(1)|$ (which cannot be sufficiently large). Eventually, the adiabatic cooling appears to be a relatively small effect, though it is still possible in this model. For example, under $\chi = 10, b = \kappa = 10, \hat{c}_p = 3.5, \hat{T}(1) = 1, \hat{T}'(1) = -0.1$, and $\hat{v}'(1) = 0.1$ [we have $\hat{v}(1) = 1$ by definition] we get for the cooling magnitude $[\hat{T}(0) - \hat{T}(1)]/\hat{T}(0) = 0.037$.

APPENDIX D: POTENTIAL VORTEX

Another familiar type of vortex in (7) and (8) is

$$\alpha = 0 \quad \text{or} \quad \frac{v_1}{v_2} = \frac{r_2}{r_1}. \tag{D1}$$

Equations (52) and (53) imply

$$\hat{T}(x) - \hat{T}(1) = \left[\hat{T}'(1) - \frac{\kappa + 4}{b + 2}\right]\frac{x^b - 1}{b} + \frac{\kappa + 4}{2(b + 2)}(1 - x^{-2}). \tag{D2}$$

Now $\hat{T}'(x) = 0$ is solved as

$$x^{-2-b} = 1 - \frac{(b + 2)T'(1)}{(w^2(1) + 1)(\kappa + 4)}. \tag{D3}$$

Hence the minimum of $\hat{T}(x)$ for $\hat{T}'(1) > 0$ can exist only for

$$\kappa < -4, \tag{D4}$$

i.e., only for radially inward flowing fluid ($c < 0$).

Now the isothermal cooling is driven by the work done for rotating cylinders. Equations (35) and (D1) imply

$$\hat{W}_\phi = 2\left(1 - x_0^{-2}\right) < 0, \tag{D5}$$

while the kinetic energy change is now larger than zero [see (67) and (D1)]. Due to this, $\hat{U}(x_0) > \hat{U}(1)$. In other respects the two scenarios of cooling (quasisolid and potential) are similar to each other: Both have roughly the same magnitude, both need small radial velocities, and both have efficiency ξ smaller than 1.

[1] G. J. Ranque, Experiments on expansion in a vortex with simultaneous exhaust of hot air and cold air, J. Phys. Radium (Paris) **4**, 112 (1933).

[2] R. Hilsch, The use of the expansion of gases in a centrifugal field as cooling process, Rev. Sci. Instrum. **18**, 108 (1947).

[3] P. A. Graham, A theoretical study of fluid dynamic energy separation, George Washington University Report No. TR-ES-721, 1972 (unpublished).

[4] A. Gutsol, The Ranque effect, Phys. Usp. **40**, 639 (1997).

[5] Y. Xue, M. Arjomandi, and R. Kelso, A critical review of temperature separation in a vortex tube, Exp. Therm. Fluid Sci. **34**, 1367 (2010).
[6] A. I. Gulyaev, Vortex tubes and the vortex effect (Ranque effect), Sov. Phys. Tech. Phys. **10**, 1441 (1966).
[7] R. T. Balmer, Pressure-driven Ranque-Hilsch temperature separation in liquids, J. Fluids Eng. **110**, 161 (1988).
[8] V. E. Finko, Cooling and condensation of gas in a vortex flow, Zh. Tekh. Fiz. **53**, 1770 (1983) [Sov. Phys. Tech. Phys. **28**, 1089 (1983)].
[9] T. Farouk, B. Farouk, and A. Gutsol, Simulation of gas species and temperature separation in the counter-flow Ranque-Hilsch vortex tube using the large eddy simulation technique, Int. J. Heat Mass Transfer **52**, 3320 (2009).
[10] J. P. Hartnett and E. R. G. Eckert, Experimental study of the velocity and temperature distribution in a high velocity vortex-type flow, Trans. ASME **79**, 751 (1957).
[11] U. Behera, P. J. Paul, K. Dinesh, and S. Jacob, Numerical investigations on flow behavior and energy separation in Ranque-Hilsch vortex tube, Int. J. Heat Mass Transfer **51**, 6077 (2008).
[12] A. Secchiaroli, R. Ricci, S. Montelpare, and V. D'Alessandro, Numerical simulation of turbulent flow in a Ranque-Hilsch vortex tube, Int. J. Heat Mass Transfer **52**, 5496 (2009).
[13] M. G. Dubinskii, Gas flow in rectilinear channels, Izv. Akad. Nauk SSSR **6**, 47 (1955) (in Russian).
[14] S. Eiamsa-ard and P. Promvonge, Review of Ranque-Hilsch effects in vortex tubes, Renew. Sustain. Energ. Rev. **12**, 1822 (2008).
[15] N. S. Torocheshnikov, I. L. Leites, and V. M. Brodyanskii, A study of the effect of temperature separation of air in a direct-flow vortex tube, Zh. Tekh. Fiz. **28**, 1229 (1958) [Sov. Phys. Tech. Phys. **3**, 1144 (1958)].
[16] R. Liew, J. C. H. Zeegers, J. G. M. Kuerten, and W. R. Michalek, Maxwell's Demon in the Ranque-Hilsch Vortex Tube, Phys. Rev. Lett. **109**, 054503 (2012).
[17] J. G. Polihronov and A. G. Straatman, Thermodynamics of Angular Propulsion in Fluids, Phys. Rev. Lett. **109**, 054504 (2012).
[18] T. S. Alekseev, The nature of the Ranque effect, J. Eng. Phys. **7**, 121 (1964) (in Russian).
[19] J. S. Hashem, A comparative study of steady and nonsteady-flow energy separators, Rensselaer Polytechnic Institute Report No. RPI-TR-AE-6504, 1965 (unpublished).
[20] M. V. Kalashnik and K. N. Visheratin, Cyclostrophic adjustment in swirling gas flows and the Ranque-Hilsch vortex tube effect, J. Exp. Theor. Phys. **106**, 819 (2008).
[21] A. P. Merkulov, A note on Alekseev's article "The nature of the Ranque effect", J. Eng. Phys. Thermophys. **8**, 474 (1965).
[22] R. Kassner and E. Knoernschild, Friction laws and energy transfer in circular flow, Wright Patterson Air Force Base Report No. PB-110936, 1948 (unpublished), Pts. I and II, available at http://www.dtic.mil/dtic/tr/fulltext/u2/a800229.pdf
[23] J. J. van Deemter, On the theory of the Ranque-Hilsch cooling effect, Appl. Sci. Res. A **3**, 174 (1952).
[24] A. J. Reynolds, Energy flows in a vortex tube, Z. Angew. Math. Phys. **12**, 343 (1961).
[25] H. Dornbrand, Theoretical and experimental study of vortex tubes, U.S. Air Force Report No. 6123, 1950 (unpublished).
[26] C. D. Pengelley, Flow in a viscous vortex, J. Appl. Phys. **28**, 86 (1957).
[27] J. M. Savino and R. G. Ragsdale, Some temperature and pressure measurements in confined vortex fields, J. Heat Transfer **83**, 33 (1961).
[28] S. Ansumali, I. V. Karlin, and H. C. Ottinger, Thermodynamic Theory of Incompressible Hydrodynamics, Phys. Rev. Lett. **94**, 080602 (2005).
[29] L. D. Landau and E. M. Lifshitz, *Fluid Mechanics*, 2nd ed., Course of Theoretical Physics Vol. 6 (Pergamon, Oxford, 1989).
[30] R. G. Deissler and M. Perlmutter, Analysis of the flow and energy separation in a turbulent vortex, Int. J. Heat Mass Transfer **1**, 173 (1960).
[31] N. Rott, On the viscous core of a line vortex, I, J. Appl. Math. Phys. **9**, 543 (1958); On the viscous core of a line vortex, II, *ibid.* **10**, 73 (1959).

[32] P. G. Bellamy-Knights, Viscous compressible heat conducting spiralling flow, Q. J. Mech. Appl. Math. **33**, 321 (1980).
[33] V. V. Kolesov and L. D. Shapakidze, Instabilities and transition in flows between two porous concentric cylinders with radial flow and a radial temperature gradient, Phys. Fluids **23**, 014107 (2011).
[34] N. Tilton, D. Martinand, E. Serre, and R. M. Lueptow, Pressure-driven radial flow in a Taylor-Couette cell, J. Fluid Mech. **660**, 527 (2010).
[35] R. M. Terrill, Flow through a porous annulus, Appl. Sci. Res. **17**, 204 (1967).
[36] R. M. Terrill, An exact solution for flow in a porous pipe, J. Appl. Math. Phys. **33**, 547 (1982).
[37] T. Colonius, S. K. Lele, and P. Moin, The free compressible viscous vortex, J. Fluid Mech. **230**, 45 (1991).
[38] R. Kumar, Study of natural convection in horizontal annuli, Int. J. Heat Mass. Transfer **31**, 1137 (1988).
[39] M. M. Rashidi, S. C. Rajvanshi, N. Kavyani, M. Keimanesh, I. Pop, and B. S. Saini, Investigation of heat transfer in a porous annulus with pulsating pressure gradient by homotopy analysis method, Arab J. Sci. Eng. **39**, 5113 (2014).
[40] J. Hona, E. H. Nyobe, and E. Pemha, Dynamic behavior of a steady flow in an annular tube with porous walls at different temperatures, Int. J. Bifurcat. Chaos **19**, 2939 (2009).
[41] M. F. Shirokov, *Physical Principles of Gasdynamics* (Fizmatgiz, Moscow, 1958) (in Russian).
[42] M. P. Silverman, The vortex tube: A violation of the second law? Eur. J. Phys. **3**, 88 (1982).
[43] W. Nusselt, Der einfluss der gastemperatur auf den wärmeübergang im rohr, Tech. Mech. Thermodyn. **1**, 277 (1930).
[44] V. S. Martynovskii and A. M. Voitko, The efficiency of the Ranque vortex tube at low pressure, Teploenergetika **2**, 80 (1961) (in Russian).
[45] L. A. Dorfman, *Hydrodynamic Resistance and the Heat Loss of Rotating Solids* (Oliver & Boyd, Edinburgh, 1963).